



1 **Silicon cycle in the Tropical South Pacific: evidence for an active**
2 **pico-sized siliceous plankton**

3 Karine Leblanc¹, Véronique Cornet¹, Peggy Rimmelin-Maury², Olivier Grosso¹, Sandra Hélias-
4 Nunige¹, Camille Brunet¹, Hervé Claustre³, Joséphine Ras³, Nathalie Leblond³, Bernard
5 Quéguiner¹

6 ¹Aix-Marseille Univ., Université de Toulon, CNRS, IRD, MIO, UM110, Marseille, F-13288,
7 France

8 ²UMR 6539 LEMAR and UMS OSU IUEM - UBO, Université Européenne de Bretagne, Brest,
9 France

10 ³UPMC Univ Paris 06, UMR 7093, LOV, 06230 Villefranche-sur-mer, France

11

12 *Correspondence to:* Karine Leblanc (karine.leblanc@univ-amu.fr)

13 **1 Abstract**

14 This article presents data regarding the Si biogeochemical cycle during two oceanographic cruises
15 conducted in the Southern Tropical Pacific (BIOSOPE and OUTPACE cruises) in 2005 and 2015.
16 It involves the first Si stock measurements in this understudied region, encompassing various
17 oceanic systems from New Caledonia to the Chilean upwelling between 8 and 34° S. Some of the
18 lowest levels of biogenic silica standing stocks ever measured were found in this area, notably in
19 the Southern Pacific Gyre, where Chlorophyll a concentrations are most depleted worldwide.
20 Integrated biogenic silica stocks are as low as 1.08 ± 0.95 mmol m⁻², and are the lowest stocks
21 measured in the Southern Pacific. Size-fractionated biogenic silica concentrations revealed a non-
22 negligible contribution of the pico-sized fraction (<2-3 μm) to biogenic silica standing stocks,
23 representing 26 ± 12 % of total biogenic silica during the OUTPACE cruise and 11 ± 9 % during
24 the BIOSOPE cruise. These results indicate significant accumulation in this size-class, which was
25 undocumented for in 2005, but has since then been related to Si uptake by *Synechococcus* cells.
26 Our Si kinetic uptake experiments carried out during BIOSOPE confirmed biological Si uptake by
27 this size-fraction. We further present diatoms community structure associated with the stock
28 measurements for a global overview of the Si cycle in the Southern Tropical Pacific.



29 **2 Introduction**

30 Siliceous phytoplankton, especially diatoms, are often associated with nutrient-rich eutrophic
31 ecosystems. However, the global budget of biogenic silica production by Nelson *et al.* (1995)
32 already pointed out the importance of these organisms in oligotrophic areas where, despite their
33 low concentration and due to the geographical extension of these systems, their silica production
34 would be comparable to the total for all areas of diatomaceous sediment accumulation combined.
35 However, studies that have documented the Si cycle in the Pacific Ocean, the largest oligotrophic
36 area of the World Ocean, mainly focused on the Equatorial region, and the northern Subtropical
37 gyre. This article presents the first set of field results from the Southern Pacific Ocean between 8
38 and 34° S spanning from New Caledonia over to the Chilean upwelling, and notably, from the most
39 Chla-depleted region at a worldwide scale (Ras *et al.*, 2008): the South Pacific Gyre (SPG).
40 Diatoms are known to contribute more importantly to primary production in meso- to eutrophic
41 systems, yet several studies have emphasized that even if they are not dominant in oligotrophic
42 regions, they may still contribute up to 10-20 % of C primary production in the Equatorial Pacific
43 (Blain *et al.*, 1997). In the oligotrophic Sargasso Sea, their contribution may be as high as 26-48 %
44 of new annual primary production (Brzezinski and Nelson, 1995) and they may represent up to 30
45 % of Particulate Organic Carbon (POC) export (Nelson and Brzezinski, 1997). In the Eastern
46 Equatorial Pacific (EEP), it has been shown that diatoms experience chronic Si-limitation along
47 the Eastern Equatorial divergence in the so-called High Nutrient Low Silicate Low Chlorophyll
48 (HNLSiLC) system (Dugdale and Wilkerson, 1998) as well as Si-Fe co-limitation (Blain *et al.*,
49 1997; Leynaert *et al.*, 2001). Furthermore, oligotrophic regions are known to experience
50 considerable variability in nutrient injections leading to episodic blooms depending on the
51 occurrence of internal waves (Wilson, 2011), meso-scale eddies (Krause *et al.*, 2010) storms
52 (Krause *et al.*, 2009), or dust deposition events (Wilson, 2003). In nitrogen (N) depleted areas,
53 punctual diatom blooms in the form of Diatom Diazotroph Associations (DDAs) are also known
54 to occur and to contribute both to new primary production (Dore *et al.*, 2008; Brzezinski *et al.*,
55 2011) but also to benefit to non-diazotrophic diatoms through secondary N-release (Bonnet *et al.*,
56 2016; Leblanc *et al.*, 2016).
57 While biogenic silica was classically associated to the largest size fractions, especially
58 microplankton, a series of recent studies have furthermore evidenced a role for picophytoplankton
59 such as *Synechococcus* in the Si cycle, showing that this ubiquitous lineage is able to take up and



60 accumulate Si (Baines et al., 2012; Ohnemus et al., 2016; Krause et al., 2017; Brzezinski et al.,
61 2017). This was evidenced in the field in the Equatorial Pacific, the Sargasso Sea, as well as in
62 culture work, suggesting a widespread diffuse role for this organism, which could be more
63 prominent in oligotrophic environments where diatoms are in low abundance. In the EEP, and
64 despite very variable cellular Si content, *Synechococcus* represented for instance 40 % of water
65 column biogenic silica (BSi) inventory compared to diatoms in 2004, and twice that of diatoms the
66 following year (Baines et al., 2012). The role of small nano-sized diatoms has also probably been
67 overlooked and we recently pointed out their general occurrence at the worldwide scale and their
68 occasional regional importance in diatom blooms (Leblanc *et al.*, 2018).

69 Here we present the first set of field results from the Southern Pacific Ocean between 8 and 34° S
70 spanning from New Caledonia over to the Chilean upwelling, and notably, from the most depleted
71 *Chla* region worldwide (Ras *et al.*, 2008), the South Pacific Gyre (SPG). Results were obtained
72 from two cruises carried out a decade apart following longitudinal sections first in the South Eastern
73 Pacific (SEP) between the Marquesas Islands and the Chilean upwelling, crossing the South Pacific
74 Gyre (BIOSOPE cruise, Oct-Dec 2004) and next in the Southern Western Pacific (SWP) between
75 New Caledonia and Tahiti (OUTPACE cruise, Feb-Apr. 2015). Very similar sampling strategies
76 and homogeneous analyses were conducted regarding the Si cycle and provide new data in this
77 under sampled region. We detail size-fractionated BSi inventories in the water column, Si export
78 fluxes, associated diatom community structure composition as well Si uptake and kinetic rates in
79 the Southern Pacific. Our key results show some of the lowest BSi stocks ever measured, which
80 may warrant for a revision of the contribution of oligotrophic areas to the global Si cycle, and
81 confirm recent findings of an active biological uptake of Si in the pico-sized fraction.

82 **3 Material and methods**

83 **3.1 Sampling strategy**

84 Results presented here encompass data from two French oceanographic cruises located in the
85 Southern Pacific Ocean (from 10 to 30° S), covering two transects with similar sampling strategies
86 of short and long duration stations. The BIOSOPE (BIo-geochemistry and Optics SOuth Pacific
87 Experiment) cruise was undertaken in 2004, while the OUTPACE cruise took place in 2015, both
88 aboard the R/V *L'Atalante*. The BIOSOPE transect was sampled between the Marquesas Islands
89 (141° W, 8° S) and Concepción (Chile) (72° W, 35° S), between October 24th and November 12th



90 2004. The OUTPACE transect was sampled between New Caledonia (159° W, 22° S) and Tahiti
91 (160° W, 20° S) between February 18th and April 3rd 2015 (Fig. 1).

92 **3.2 Hydrology**

93 Water sampling and measurements of temperature and salinity were performed using a SeaBird
94 SBE 911plus CTD/Carousel system fitted with an in situ fluorometer and 24 Niskin bottles. More
95 details about the BIOSOPE cruise strategy are given in the Biogeoscience special issue
96 introductory article by Claustre et al., (2008) while the OUTPACE cruise strategy is detailed in
97 Moutin et al. (2017). Euphotic layer depths (Z_e) were calculated as described in Raimbault et al.
98 (2008) and Moutin et al. (2018).

99 **3.3 Inorganic nutrients**

100 Nutrients were collected in 20 mL PE vials and analyzed directly on a SEAL Analytical auto-
101 analyzer following Aminot and K erouel (2007) on board during BIOSOPE and at the laboratory
102 during OUTPACE from frozen (-20°C) samples.

103 **3.4 Particulate Organic Carbon (POC)**

104 Seawater samples (~2 L) were filtered through pre-combusted 25 mm GF/F filters, dried at 60 °C
105 and stored in 1.5 mL eppendorfs PE tubes. Particulate Organic Carbon (POC) was analyzed on a
106 CHN elemental analyzer (Perkin Elmer, 2400 series).

107 **3.5 Total Chlorophyll *a* (TChl*a*)**

108 For pigment analyses, 2 L of seawater were filtered through 25 mm GF/F filters and stored in liquid
109 nitrogen and -80°C until processing. Extraction was done in 3 mL 100% methanol, followed by
110 sonication and clarification by filtration on a new GF/F filter. Extracted pigments (Chl*a* and
111 fucoxanthin) were then analyzed by HPLC (High Performance Liquid Chromatography) according
112 to the procedure detailed in Ras et al. (2008).

113 **3.6 Particulate Biogenic and Lithogenic Silica (BSi/LSi)**

114 Samples were collected for silicon stocks as particulate biogenic and lithogenic silica (BSi and LSi)
115 and dissolved orthosilicic acid (Si(OH)₄) similarly on both cruises. For BSi/LSi, between 1.5 and
116 2.5 L Niskin samples were filtered through cascading polycarbonate 47 mm filters. During



117 BIOSOPE, whole samples were filtered through three cascading filters of 0.2, 2, and 10 μm . During
118 OUTPACE, the size-fractionation used was 0.4 and 3 μm respectively. Filters were rinsed with 0.2
119 μm filtered seawater, folded in 4 and placed in Petri dishes and dried overnight at 60°C. Filters
120 were then stored at room temperature and analyzed in the laboratory. BSi and LSi were measured
121 using Paasche (1973) as modified by Nelson et al. (1989): BSi and LSi were extracted on the same
122 filter after successive basic and acid treatments. BSi was extracted during a hot sodium hydroxide
123 (NaOH 0.2 N) attack (60 min), which converted BSi into the dissolved orthosilicic acid form.
124 $\text{Si}(\text{OH})_4$ was then quantified using the Strickland and Parsons (1972) spectrophotometric method.
125 After the first basic attack, filters were rinsed free of remaining $\text{Si}(\text{OH})_4$ and dried again at 60°C.
126 LSi, preserved in the sample, was then treated with hydrofluoric acid (HF 2.9 N) for 48 h. In the
127 same way, LSi was measured through quantification of the dissolved $\text{Si}(\text{OH})_4$ form. Precisions for
128 BSi and LSi measurements were 4 and 6 nmol L^{-1} respectively (twice the standard deviation of
129 blanks). It has been demonstrated that for coastal samples, significant leaching of orthosilicic acid
130 from LSi could occur during the first NaOH attack (up to 15 %) (Ragueneau and Tréguer, 1994).
131 This is particularly the case when high LSi concentrations are present. Kinetic assays of orthosilicic
132 acid were conducted in some samples from the Marquesas, Gyre, East-Gyre and near Upwelling
133 stations during BIOSOPE, but results revealed negligible LSi interferences after an extraction time
134 of 60 min.

135 Biogenic silica export fluxes were determined from drifting sediment traps deployed at three depths
136 (153, 328, 519 m) at the three long duration stations of the OUTPACE cruise. Each trap was
137 deployed for 4 consecutive days, and the average daily flux was quantified by adding the amount
138 of dissolved Si in each trap to the measured BSi concentration to account for BSi dissolution in the
139 trap samples during storage. This step proved necessary, as BSi dissolution ranged between 16 and
140 90 % depending on the samples.

141 **3.7 Si bulk and specific uptake rates ($\rho\text{Si}/\text{VSi}$)**

142 During BIOSOPE, dawn-to-dawn in situ Si uptake experiments were performed using an immersed
143 production line, at six incubation depths (50 %, 25 %, 15 %, 8 %, 4 % and 1 % light level). Seawater
144 (275 mL) samples were spiked with 632 Bq of radiolabeled ^{32}Si -silicic acid solution (specific
145 activity of 23.46 $\text{kBq } \mu\text{g-Si}^{-1}$). For all samples, $\text{Si}(\text{OH})_4$ addition did not exceed 0.4 % of the initial
146 concentration. After incubation, samples were filtered through cascading polycarbonate



147 membranes (0.2, 2 and 10 μm , 47 mm). Filters were rinsed with filtered (0.2 μm) seawater, and
148 placed in scintillation vials. The ^{32}Si uptake was measured in a Packard 1600-TR scintillation
149 counter by Cerenkov effect, following the method described by Tréguer and Lindner (1991) and
150 Leynaert (1993). Precision of the method averages 10 % to 25 % for the less productive station.

151 **3.8 Si uptake kinetics**

152 Samples used were collected from the same Niskin bottles as those used for in situ incubation at
153 the depth of the Chl*a* maximum. Six samples from each depth received non-radioactive $\text{Si}(\text{OH})_4$
154 additions so that concentrations increased respectively by 0, 1.1, 2.3, 4.5, 13.6, 36.4 μM . Bottles
155 were incubated on board in a deck incubator for 8h using neutral nickel screens. Samples were
156 thereafter treated as described for in situ samples. Kinetic parameters K_s and V_{max} were calculated
157 by fitting the data to a hyperbolic curve using the Sigmaplot® hyperbola fit.

158 **3.9 Siliceous phytoplankton determinations**

159 Seawater samples were preserved with acidified Lugol's solution and stored at 4°C. A 500 mL
160 aliquot of the sample was concentrated by sedimentation in glass cylinders for six days. Diatoms
161 were counted following the method described by Gomez et al. (2007).

162 **3.10 Phytoplankton net samples**

163 During the OUTPACE cruise, additional phyto-net hauls were undertaken at each site integrating
164 the 0-150 m water column, except at stations LD-C, 14 and 15 where they integrated the 0-200 m
165 water column due to the presence of a very deep Deep Chlorophyll *a* Maximum (DCM). Samples
166 were preserved in acidified lugol, and observed in a Sedgewick-rafter chamber. A semi-quantitative
167 species list (dominant, common, rare) was established.

168 **4 Results**

169 **4.1 Hydrological systems and nutrient availability**

170 The hydrological structures crossed during the two transects have been carefully detailed in
171 companion papers (Claustre et al., 2008; Moutin et al., 2018; Fumenia et al., 2018) and will not be
172 presented in detail here. For the sake of clarity in the present article, main hydrological systems are
173 described as follows. During the BIOSOPE cruise, five main hydrological systems were defined



174 from West to East: the HNLC system comprising long duration (LD) stations MAR (Marquesas)
175 and HNL and station 1; the South Tropical Pacific (STP) system from stations 2 to 6; the central
176 part of the South Pacific Gyre (SPG) from station 7 to 13 including the LD station GYR; the Eastern
177 Gyre HNLC area from stations 14 to 19 including LD station EGY (Eastern Gyre); and the coastal
178 Peru-Chile Upwelling system from station 20 to 21 including LD stations UPW and UPX. During
179 OUTPACE, two main systems were encountered, from West to East, the MA (Melanesian
180 Archipelago) from stations 1 to 12 and including LD stations A and B, and the South Pacific Gyre
181 (SPG) from stations 13 to 15 and including LD station C.

182 During both cruises, eutrophic to ultra-oligotrophic conditions were encountered. During
183 OUTPACE, Si(OH)_4 concentrations were $<1 \mu\text{M}$ at all stations in the surface layer, with values as
184 low as $0.3\text{-}0.6 \mu\text{M}$ at 5 m depth at certain stations (Fig. 2). The $1 \mu\text{M}$ isoline was centered at ~ 100
185 m in the western part of the MA, and deepened to ~ 200 m in the SPG. Concentrations at 300 m
186 were quite low ($<2 \mu\text{M}$) over the entire transect. Nitrate concentrations were similarly depleted in
187 the surface layer, with values $<0.05\text{-}0.1 \mu\text{M}$ in the first 80 m in the western part of the MA (until
188 station 6), which deepened to 100 m over the rest of the transect. Yet nitrate concentrations
189 increased with depth more rapidly than orthosilicic acid, reaching concentrations close to $7 \mu\text{M}$ at
190 300 m depth.

191 Phosphate was below detection limits in the western part of the MA (stations 1 to 11, and station
192 B) over the first 50 m, but increased to values comprised between 0.1 and $0.2 \mu\text{M}$ in the SPG.
193 Concentrations only increased to $0.6\text{-}0.7 \mu\text{M}$ at 300 m depth.

194 During BIOSOPE, both the nitracline and phosphacline extended very deeply (~ 200 m) in the
195 regions of the STP, SPG and Eastern Gyre (Fig. 3). They surfaced at both ends of the transect in
196 the upwelling system and near the Marquesas Islands, but contrary to nitrate which was severely
197 depleted, phosphate was never found $<0.1 \mu\text{M}$ in the surface layer (except at the subsurface at site
198 14). The distribution of orthosilicic acid concentrations were less clearly contrasted, with general
199 surface values comprised between 0.5 and $1 \mu\text{M}$ in the surface layer, except in the western part of
200 the transect from station 1 to the GYR station, and in the upwelling system, where concentrations
201 were $> 1 \mu\text{M}$ and up to $8.9 \mu\text{M}$ at the surface and increasing rapidly with depth.



202 **4.2 Total Chl*a* and fucoxanthin distribution**

203 Total Chl*a* (TChl*a*) distributions are presented for both cruises along longitudinal transects together
204 with fucoxanthin concentrations, a diagnostic pigment for diatoms (Fig. 4a, b). During OUTPACE,
205 the Melanesian Archipelago system was clearly enriched in TChl*a* compared to the South Pacific
206 Gyre and showed non-negligible concentrations in surface layers as well as a pronounced DCM
207 reaching up to 0.45 $\mu\text{g L}^{-1}$ at station 11. The observed DCM progressively deepened eastwards,
208 from 70 m depth at LD-A to 108 m at station 12. The DCM depth generally closely followed the
209 euphotic layer depth (Z_{eu}) or was located just below it. The highest surface concentrations were
210 found at stations 1 to 6, between New Caledonia and Vanuatu (0.17 to 0.34 $\mu\text{g L}^{-1}$) while the SPG
211 surface water stations showed a depletion in Chl*a* (0.02 to 0.04 $\mu\text{g L}^{-1}$). A DCM subsisted in this
212 region, but was observed to be deeper (125 to 150 m) and of lower amplitude (0.17 to 0.23 $\mu\text{g L}^{-1}$)
213 than in the MA region. Fucoxanthin concentrations closely followed the DCM, but were extremely
214 low over the entire transect, with a maximum concentration of 17 ng L^{-1} in the MA and of 4 ng L^{-1}
215 in the SPG.

216 The BIOSOPE cruise evidenced a very similar Chl*a* distribution in the central SPG than during the
217 OUTPACE cruise, with extremely low surface concentrations and a very deep Chl*a* maximum
218 located between 180 - 200 m ranging between 0.15 and 0.18 $\mu\text{g L}^{-1}$. On both sides of the central
219 SPG, the DCM shoaled towards the surface at the MAR station at the western end of the transect
220 (0.48 $\mu\text{g L}^{-1}$ at 30 m) and at the UPW station at the eastern end of the transect (3.06 $\mu\text{g L}^{-1}$ at 40
221 m). Fucoxanthin concentrations did not exceed 9 ng L^{-1} at any station between the STP and the
222 Eastern Gyre (between LD-HNL and station 17), thus showing ranges similar to the OUTPACE
223 cruise measurements. Fucoxanthin increased moderately at the MAR station (85 ng L^{-1}), while it
224 peaked in the Peru-Chile upwelling system with concentrations reaching 1,595 ng L^{-1} at LD-UPW
225 but remained much lower at the LD-UPX station (200 ng L^{-1}).

226 **4.3 Total and size-fractionated Biogenic and Lithogenic Silica standing stocks**

227 Total Biogenic silica (BSi) concentrations were extremely low during the OUTPACE cruise (Fig.
228 5a) and ranged between 2 and 121 nmol L^{-1} in the surface layers, with an average concentration of
229 17 nmol L^{-1} . Similarly to TChl*a* and fucoxanthin, the highest BSi levels were encountered over the
230 MA, with peak values mostly found at the surface, at stations 1 and 2 and from stations 4 to 7, and
231 with very moderate increases at depth (stations 5 and 10). The average BSi concentration decreased



232 from 20 to 8 nmol L⁻¹ from the MA to the SPG. In the SPG, maximum BSi levels were found at
233 the DCM, between 125 and 150 m. Total Lithogenic Silica (LSi) concentrations were measured in
234 a very similar range (Fig. 5b), between 2 and 195 nmol L⁻¹, with a peak value at station 2 at 100 m.
235 Also, LSi was ranged from 5 to 30 nmol L⁻¹ over the transect, with highest values observed close
236 to 100 m, while averaged concentrations followed the same trend as BSi, decreasing from 16 to 9
237 nmol L⁻¹ between the MA and the SPG.

238 During the BIOSOPE cruise, three main regions could be differentiated: a first region covering the
239 ultra-oligotrophic central area from station 1 to station 20, where average BSi concentrations were
240 as low as 8 nmol L⁻¹ (Fig. 5c). At the western end of the transect, the first three stations in the
241 vicinity of the Marquesas Islands had higher concentrations with average values of 104 nmol L⁻¹.
242 The eastern end of the transect, located in the Peru-Chile Upwelling system, displayed much higher
243 and variable values, averaging 644 nmol L⁻¹, with a maximum concentration of 2,440 nmol L⁻¹ at
244 the UPW station at 60 m. At both ends of the transect, siliceous biomass was mainly distributed in
245 the upper 100 m. Lithogenic silica followed the same trends (Fig. 5d), with extremely low values
246 over the central area (average of 7 nmol L⁻¹) with a few peaks close to 30 nmol L⁻¹ (stations 12 and
247 EGY). LSi was again higher at both ends of the transect but with less amplitude than BSi, with
248 average values of 26 nmol L⁻¹ close to the Marquesas, and of 57 nmol L⁻¹ in the coastal upwelling
249 system. The maximum values close to 150 nmol L⁻¹ were associated to the BSi maximums at the
250 UPW sites.

251 Size-fractionated integrated BSi stocks were calculated for both cruises over the 0-125 m layer,
252 except for the BIOSOPE cruise at station UPW1, which was only integrated over 50 m and at
253 stations UPX1 and UPX2 which were integrated over 100 m (Fig. 6a, b, Appendix 1). Total BSi
254 stocks were similarly very low in the ultra oligotrophic central gyre and averaged 1 mmol Si m⁻²
255 during both cruises. During BIOSOPE, the stocks measured close to the Marquesas averaged 9.85
256 mmol Si m⁻² (with a peak of 24.12 mmol Si m⁻² at the MAR station). On the eastern end of the
257 transect, stocks increased to a peak value of 142.81 mmol Si m⁻² at the UPW2 station and averaged
258 65.68 mmol Si m⁻² over the coastal upwelling system. Size-fractionation was only carried out at
259 the long duration stations, but showed an overall non negligible contribution of the pico-sized
260 fraction (0.2-2 μm) to BSi standing stocks of 11 ± 9 %. This contribution of the pico-size fraction
261 to integrated siliceous biomass was highest at the GYR, EGY and UPX1 stations reaching 25, 18
262 and 24 % respectively.



263 During OUTPACE, integrated BSi stocks ranged between 1.25 and 4.11 mmol Si m⁻² over the MA,
264 and decreased to 0.84 to 1.28 mmol Si m⁻² over the SPG (Fig. 6c, Appendix 2). Here, size-
265 fractionation was conducted at all sites and the contribution of the 0.4 - 3 μm, which will be
266 assimilated to the pico-size fraction hereafter, was higher than during BIOSOPE, with an average
267 contribution of 26 ± 12 %. The importance of the picoplanktonic Si biomass was higher in the SPG
268 (36 ± 12 %) than over the MA (22 ± 10 %).

269 4.4 Si uptake rates and kinetic constants

270 Si uptake rate measurements using the ³²Si radioactive isotope were only conducted during the
271 BIOSOPE cruise. The same size-fractionation was applied to production and kinetic experiment
272 samples. Vertical profiles of gross production rates (pSi) confirm the previous stock information
273 and show that the most productive stations, in decreasing order of importance, are the UPW, UPX
274 and MAR stations (Fig. 7a), with 1.98, 1.19 and 0.22 μmol Si L⁻¹ d⁻¹ at 10 m respectively. Si uptake
275 rates remained below 0.015 μmol Si L⁻¹ d⁻¹ at central HNLC and oligotrophic stations HNL, EGY
276 and GYR. Si uptake rates in the picoplanktonic size fraction showed similar trends (Fig. 7b),
277 despite higher values at UPX (0.076 μmol Si L⁻¹ d⁻¹) than at UPW (0.034 μmol Si L⁻¹ d⁻¹). Uptake
278 rates in that size fraction were intermediate at the MAR station with maximum value of 0.005 μmol
279 Si L⁻¹ d⁻¹, while it remained below 0.001 μmol Si L⁻¹ d⁻¹ at the central stations. Specific Si uptake
280 (VSi normalized to BSi) rates for the picoplanktonic size fraction were even more elevated and
281 reached maximum values of 3.64, 1.32, 0.75, 0.37 and 0.14 d⁻¹ at the UPW, UPX, HNL, EGY and
282 MAR stations respectively. Total specific Si uptake rates were extremely high in the coastal
283 upwelling system, with values of 2.57 and 1.75 d⁻¹ at UPX and UPW respectively, and lower but
284 still elevated values at the MAR station (0.75 d⁻¹). VSi at the central stations (HNL, EGY, GYR)
285 were moderate to low and ranged between 0.02 and 0.24 d⁻¹.

286 Total ΣpSi reached 52.4 mmol Si m⁻² d⁻¹ at UPW2 station, an order of magnitude higher than the
287 rate measured at the MAR station (5.9 mmol Si m⁻² d⁻¹) and 3 orders of magnitude higher than at
288 EGY, where the lowest value was obtained (0.04 mmol Si m⁻² d⁻¹). Integrated picoplanktonic Si
289 uptake rates (ΣpSi for 0.2-2 μm) were highest at both upwelling stations (Table 1), followed by the
290 MAR station. The relative average contribution of the picoplanktonic size fraction to total Si uptake
291 rates was highest at the central stations (32 % at GYR, 19 % at EGY and 11 % at HNL) while it
292 was lowest on both ends of the transect (5 % at MAR, and 3 and 7 % at UPW and UPX stations).



293 Si uptake kinetic experiments were conducted at some long duration stations at the surface and/or
294 depth of the DCM depending on the location of biomass. Results for the picoplanktonic fraction
295 clearly indicate an active biological uptake (Fig. 8), generally following hyperbolic uptake kinetics.
296 The hyperbolic curve fitting failed for only 2 out of the 8 kinetic uptake experiments performed on
297 the 0.2-2 μm size-fraction (at the DCM at the HNL station and at the surface at the UPX station).
298 Maximum theoretical specific uptake rates (V_{max}) values were high, ranging from 1.9 d^{-1} at the
299 MAR station to 6.1 d^{-1} at the surface at the UPX station. Half-saturation constants (K_S) were also
300 elevated ranging from 5.4 μM at the MAR station to as much as 38.3 μM at the UPX station and
301 in all cases much higher than ambient $\text{Si}(\text{OH})_4$ concentrations.

302 **4.5 Diatom distribution and community structure**

303 Microscopical examinations confirmed the presence of diatoms at every station during both cruises.
304 Diatoms were found in very low abundances during the OUTPACE cruise and only reached
305 maximum values of 20,000-30,000 cells L^{-1} on two occasions, at stations LD-B at the surface and
306 at station 5 at the DCM (Fig. 9a). Mean diatom concentrations in the MA at the surface were 4,440
307 $\pm 7,650$ cells L^{-1} while at the DCM, mean concentrations were about 2-fold lower ($2,250 \pm 4,990$
308 cells L^{-1}). Diatom abundance decreased dramatically in the SPG, with values as low as 25 ± 19
309 cells L^{-1} at the surface layers and 145 ± 54 cells L^{-1} at the DCM. The richness of diatoms was higher
310 in the MA than in the SPG, with an average number of taxa of respectively 9 ± 4 and 2 ± 1 in the
311 surface layer (Fig. 9b). The richness increased at the DCM level, with 12 ± 8 taxa in the MA and
312 5 ± 1 taxa in the SPG. Diatom contribution to biomass was accordingly extremely low and remained
313 below 3 % (Fig. 9c). The diatom contribution to C biomass increased more significantly only at
314 two stations: at station LD-B (9 % at the surface) and at station 5 where the maximum value for
315 the cruise was observed (11.5 % at the DCM).

316 During BIOSOPE, the central stations showed a record low diatom abundance with less than 100
317 cells L^{-1} from stations 2 to EGY (Fig. 10). The eastern part of the SPG and the HNL stations were
318 characterized by slightly higher abundances (from 100 to 1,000 cells L^{-1}), followed by the UPX
319 station, where abundances were similar to the MAR station at the surface ($\sim 25,000$ cells L^{-1}).
320 Highest abundances were observed at the UPW, with bloom values of 256,000 cells L^{-1} on average
321 (with a peak abundance of 565,000 cells L^{-1} at the surface). Similar results compared to OUTPACE
322 showed an extremely low richness at all central stations (data not shown) with on average 3 ± 2



323 diatom taxa, while richness increased at the western HNLC region with 13 ± 4 taxa at the MAR
324 and HNL stations. Richness was highest at the UPW station with 20 ± 4 taxa and decreased again
325 at the UPX station (5 ± 3).

326 The dominant diatom species for each system sampled over the course of the two cruises are
327 summarized in Table 1 and Appendix 3. During OUTPACE, very similar species were encountered
328 in both regions and were mainly dominated by pennate species such as *Pseudo-nitzschia* spp., *P.*
329 *delicatissima*, *Cylindrotheca closterium* and *Mastogloia woodiana*. However, Diatom-Diazotroph
330 Associations (DDAs) such as *Rhizosolenia styliformis*, *Climacodium frauenfeldianum* and
331 *Hemiaulus hauckii* were more abundantly found in the MA. Other siliceous organisms such as
332 radiolaria were also more abundant in the SPG and at LD-B than in the MA (Appendix 3). Overall
333 microplanktonic diazotroph abundance were much higher over the MA than in the gyre, with a
334 predominance in plankton nets of *Trichodesmium*, *Richelia intracellularis* (alone or in DDAs),
335 *Crocospaera* and other filamentous cyanobacteria such as *Katagnymene* (Appendix 3).

336 Diatom community structure for the BIOSOPE cruise has already been discussed extensively in
337 Gomez et al. (2007). In summary, the stations characterized by medium diatom abundances such
338 as MAR, HNL, 18, 20 and EGY (Fig. 10) were mainly dominated by the pennate diatom *Pseudo-*
339 *nitzschia delicatissima* in particular at the MAR station, where it represented on average 90 % of
340 all diatoms over the 0-100 m layer. Extremely low abundance stations (< 200 cells L^{-1}) from the
341 middle of the SPG (stations 2 to 14) did not show any consistent community, with varying dominant
342 species across stations and along vertical profiles as well. Maximum abundances at these sites were
343 consistently found at depth, between 100 and 200 m. In the Peru-Chile upwelling, diatom
344 community structure was mostly dominated by small and colonial centric species such as
345 *Chaetoceros compressus* and *Bacteriastrum* spp. at the UPW station where abundances were
346 highest ($565,000$ cells L^{-1}) and such as *Skeletonema* sp. and *Thalassiosira anguste-lineata* at the
347 UPX station where abundances decreased to $10,000$ - $40,000$ cells L^{-1} . In this system, the highest
348 abundances were found in the first 10 m.

349 **4.6 Si export fluxes**

350 Particulate silica export fluxes were measured from drifting trap deployments at each long duration
351 station during OUTPACE and are presented in Table 3. BSi daily export fluxes below the mixed
352 layer at 153, 328 and 529 m were extremely low at all sites, with lowest values at site A (0.5 to 0.1



353 $\mu\text{mol Si m}^{-2} \text{d}^{-1}$), highest at site B (3 to 5 $\mu\text{mol Si m}^{-2} \text{d}^{-1}$) and intermediate at site C (0.5 to 2 μmol
354 $\text{Si m}^{-2} \text{d}^{-1}$).

355 **5 Discussion**

356 **5.1 Si budgets for the South Pacific**

357 In the following section, values from previous studies are compared (Table 4) with the results
358 obtained across this under-studied region of the Pacific Ocean, which is characterized by the most
359 oligotrophic and *Chla* depleted waters worldwide (Ras et al., 2008). On one hand, size-fractionated
360 biomass and export fluxes were obtained during the OUTPACE program, while on the other hand,
361 size-fractionated production and biomass budgets were quantified during the BIOSOPE program.
362 Regarding values obtained at both ends of the BIOSOPE transects, i.e. in the Peru-Chile upwelling
363 system and in the HNLC system surrounding the Marquesas Islands, $\Sigma\rho\text{Si}$ rates compare well with
364 previous studies from other similar regions (Table 4). Integrated Si production rates at the UPW
365 stations are in the middle range (42-52 $\text{mmol Si m}^{-2} \text{d}^{-1}$) of what was previously found in coastal
366 upwellings. Values are however almost double to what was previously observed in the Peru
367 upwelling by Nelson et al. (1981), although less productive than the Monterey Bay and Baja
368 Californian upwelling systems (Nelson and Goering, 1978; Brzezinski et al., 1997). For oceanic
369 HNLC areas, values obtained (0.8 to 5.6 $\text{mmol Si m}^{-2} \text{d}^{-1}$) cover the range of rates measured in
370 HNLC to mesotrophic systems of the North Atlantic, Central Equatorial Pacific and Mediterranean
371 Sea. However, integrated rates obtained for the oligotrophic area of the South Eastern Pacific Gyre
372 are to our knowledge among the lowest ever measured. Indeed, values range from 0.04 to 0.20
373 $\text{mmol Si m}^{-2} \text{d}^{-1}$, they are thus lower than average values previously measured at BATS and
374 ALOHA stations (0.42 and 0.19 $\text{mmol Si m}^{-2} \text{d}^{-1}$ respectively) (Brzezinski and Kosman, 1996;
375 Nelson and Brzezinski, 1997; Brzezinski et al., 2011). However, they are similar to measurements
376 performed in autumn (0.04-0.08 $\text{mmol Si m}^{-2} \text{d}^{-1}$) in a severely Si-limited regime of the North
377 Atlantic (Leblanc et al., 2005b). Previous studies have evidenced limitation of diatom Si production
378 by Si (Leynaert et al., 2001), but more recently evidence of co-limitation by both Si and Fe was
379 found in the central Equatorial Pacific (Brzezinski et al., 2008). This would be a more than likely
380 scenario for the SPG, given the very low silicic acid (Fig.2 & 3) and Fe concentrations (0.1 nM
381 and ferricline below 350 m depth, Blain et al., 2008) measured during both cruises. The
382 approximate surface area of mid-ocean gyres was estimated to be $1.3 \times 10^8 \text{ km}^2$ (representing



383 approximately 1/3 of the global ocean) yielding a global contribution of only 26 Tmol Si y⁻¹ gross
384 silica production, i.e. approximately 9-13% of the budget calculated for the global ocean of 240
385 Tmol Si y⁻¹ according to Nelson et al. (1995). This budget has been recently revised down to 13
386 Tmol Si y⁻¹ reducing the contribution of subtropical gyres to 5-7% of global marine silica
387 production (Brzezinski et al., 2011; Tréguer and de La Rocha, 2013). However, the range provided
388 in Nelson et al. (1995) in the calculation of their global Si production fluxes for mid-ocean gyres
389 was of 0.2 – 1.6 mmol m⁻² d⁻¹. Our values would, once again, lower the contribution of these vast
390 oceanic regions to global Si production, although the present data is only based on two production
391 station measurements and warrants further measurements for this region. Nevertheless, it can be
392 expected that the most ultra-oligotrophic region of the world ocean would contribute even less to
393 total Si production than the other oligotrophic systems listed in Table 4 and that in particular, the
394 Si production in the ultra-oligotrophic Southern Tropical Gyre would be lower than the Northern
395 Tropical Gyre.

396 Integrated Si biomass also reflects the very low contribution of diatoms in this system, which was
397 more than 2-fold lower in the South Pacific Gyre than in the Melanesian Archipelago (Table 5).
398 In the SPG, the lowest Si stocks were measured (~1 mmol Si m⁻²), and were similar to lower-end
399 values found in the ultra-oligotrophic Eastern Mediterranean Basin in autumn and in other
400 oligotrophic areas of the North Pacific Subtropical Gyre and of the Sargasso Sea (Table 5 and
401 references therein). It is probable that ΣpSi production and BSi stocks could have been slightly
402 higher less than a month earlier in the season on the western part of the OUTPACE transect in the
403 MA. Indeed, the satellite-based temporal evolution of Chl*a* at stations LD-A and LD-B showed
404 decreasing concentrations at the time of sampling (de Verneil et al., 2018), while the situation did
405 not show any temporal evolution for the SPG, thus suggesting that the biogenic silica budget for
406 this area is quite conservative under a close to steady-state situation.

407 Lastly, our Si export flux measurements by drifting sediment traps are the lowest ever measured
408 and are about two orders of magnitude lower than those from other oligotrophic sites such as BATS
409 in the Atlantic or ALOHA in the Pacific Ocean (Table 6). They represent a strongly negligible
410 fraction of surface Si stocks, implying no sedimentation at the time of sampling, and that active
411 recycling and grazing occurred in the surface layer. Indeed, surface temperatures higher than 29°C
412 at all long duration sites, may favor intense dissolution in the upper layer, while active zooplankton
413 grazing was also documented, removing between 3 and 21% of phytoplankton stocks daily (Carlotti



414 et al., 2018). The virtual absence of silica export from the surface layer well agrees with the
415 conclusion of Nelson *et al.* (1995) that no siliceous sediment is accumulating beneath the central
416 ocean gyres.
417

418 **5.2 Siliceous plankton community structure in the South Tropical Pacific**

419 The main feature observed during OUTPACE was a bi-modal distribution of diatom communities,
420 either at the surface and/or at the DCM level depending on stations, which deepened towards the
421 East, following the increasing oligotrophy gradient, similarly to what was previously described in
422 the Mediterranean Sea (Crombet *et al.*, 2011). A similar feature, showing a particularly deep DCM,
423 up to 190 m in the SPG at 1.2-fold the euphotic depth (Ras *et al.*, 2008), was observed during
424 BIOSOPE, revealing a known strategy for autotrophic plankton cells in nutrient depleted waters to
425 stay at the depth where the best light vs nutrient ratio is obtained (Quéguiner, 2013).

426 If the presence of DCMs in oligotrophic mid-ocean gyres are well known, associated to the
427 dominance of small pico-sized phytoplankton (Chavez *et al.*, 1996), studies documenting
428 phytoplankton community structure in the South Tropical Pacific Ocean, an area formerly called a
429 « biological desert », are still very scarce. In the review of planktonic diatom distribution by
430 Guillard and Kilham (1977) referencing biocenoses for all main oceanic water bodies and for which
431 thousands of articles were processed, the diatom composition for the South Tropical region was
432 referred to as « No species given (flora too poor) ». Since then only a few studies mentioning
433 phytoplankton community structure, mostly located along the equator were published, such as
434 Chavez *et al.* (1990); Chavez *et al.* (1991); Iriarte and Fryxell (1995); Kaczmarska and Fryxell
435 (1995); and Blain *et al.* (1997). In Semina and Levashova (1993) some biogeographical distribution
436 of phytoplankton including diatoms is given for the entire Pacific region, yet the Southern tropical
437 region is limited to more historical Russian data and rely on very few stations. The only diatom
438 distribution for the South Tropical Gyre was published for the present data set by Gomez *et al.*
439 (2007) in the BIOSOPE special issue. Hence the present data contributes to documenting a severely
440 understudied, yet vast area of the world ocean.

441 The oceanic regions covered during both cruises may be clustered into three main ecological
442 systems with relatively similar diatom community structures: the nutrient-rich coastal upwelling
443 system near the Peru-Chile coast, where diatom concentrations exceeded 100,000 cells L⁻¹, the Fe-
444 fertilized areas of the Melanesian Archipelago and West of Marquesas Islands, where



445 concentrations could locally exceed 10,000 cells L⁻¹, and all the other ultra-oligotrophic regions
446 (mainly the South Pacific Gyre system) characterized by extremely low diatom abundances,
447 usually <200 cells L⁻¹.

448 The upwelling area was characterized by a distinct community, not found in the other regions,
449 composed of typical neritic and centric colonial species such as *Skeletonema* sp., *Bacteriastrium*
450 spp., *Chaetoceros compressus*, *Thalassiosira subtilis* and *T. anguste-lineata*. These first three
451 species were already documented as abundant in the Chile upwelling by Avaria and Munoz (1987),
452 whereas *T. anguste-lineata* was reported along the Chilean coast from 20°S to 36°S (Rivera et al.,
453 1996) and was also documented in the upwelling system West of the Galapagos Islands (Jimenez,
454 1981). The highest pSi production values were measured at the offshore UPW station where
455 *Bacteriastrium* spp. and *Chaetoceros compressus* co-occurred as the two dominant species, whereas
456 pSi rates were halved at the closest coastal station UPX, associated to lower abundances of diatoms,
457 with co-occurring dominance by *Skeletonema* sp. and *Thalassiosira anguste-lineata*.

458 The HNLC regions off the Marquesas Islands (MAR) and in the Eastern Gyre (stations 14-20,
459 BIOSOPE) and the oligotrophic region (N-depleted but Fe-fertilized region of the MA), with
460 bloom situations at stations 5 and LD-B (OUTPACE), showed strong similarities in terms of
461 diatom community structure and were all mainly dominated by the medium-sized pennate diatoms
462 of the *Pseudo-nitzschia delicatissima/subpacificica* species complex. These pennate species are
463 commonly reported for the Central and Equatorial Pacific Ocean (Guillard and Kilham, 1977;
464 Iriarte and Fryxell, 1995; Blain et al., 1997). During BIOSOPE, *Pseudo-nitzschia delicatissima*
465 were often seen forming « needle balls » of ~100 µm diameter which suggests an anti-grazing
466 strategy from micro-grazers (Gomez et al., 2007), a strategy already described by several authors
467 (Hasle, 1960; Buck and Chavez, 1994; Iriarte and Fryxell, 1995). Predominance of pennate diatoms
468 over centrics has previously been observed in the N-depleted environment of the Equatorial Pacific
469 (Blain et al., 1997; Kobayashi and Takahashi, 2002), and could correspond to an ecological
470 response to diffusion-limited uptake rates, favoring elongated shapes, as suggested by Chisholm
471 (1992). Furthermore, net samples from the OUTPACE cruise showed a numerically dominant
472 contribution of *Cylindrotheca closterium* over 0-150 m at most stations of the MA (Appendix 3),
473 with a strong dominance at LD-B, even though their contribution to biomass is minor given their
474 small size. *Pseudo-nitzschia* sp. and *Cylindrotheca closterium* have been shown to bloom upon Fe-
475 addition experiments (Chavez et al., 1991; Fryxell and Kaczmarska, 1994; Leblanc et al., 2005a;



476 Assmy et al., 2007) and may reflect the significantly higher dissolved Fe concentrations measured
477 in the MA (average 1.9 nM in the first 100 m) compared to the SPG (0.3 nM) (Guieu et al., in rev).
478 In the Equatorial Pacific, Fe-amendment experiments evidenced the rapid growth of *Cylindrotheca*
479 *closterium*, with a high doubling rate close to 3 d⁻¹ (Fryxell and Kaczmarska, 1994), which can
480 explain why this species is often numerically dominant.

481 Fast growing colonial centric diatoms such as *Chaetoceros* spp. were notably absent from the MA,
482 except at stations 5 and LD-B, where mesoscale circulation increased fertilization (de Verneil et
483 al., 2018) and allowed a moderate growth (observed in both Niskin samples and net hauls),
484 resulting in an increased contribution of diatoms to total C biomass of approximately 10% (Fig.
485 9c). Other typical bloom species such as *Thalassiosira* spp. were completely absent from the
486 species from the Niskin samples but observed at low abundance in some net haul samples.
487 Nonetheless, very large centrals typical of oligotrophic waters such as *Rhizosolenia calcar-avis*
488 (Guillard and Kilham, 1977) were present in low numbers at all stations and in all net hauls, and
489 represented a non-negligible contribution to biomass despite their low abundance.

490 One difference with the N-replete Marquesas HNLC system was that the hydrological conditions
491 of the MA were highly favorable for the growth of diazotrophs, with warm waters (>29°C),
492 depleted N in the surface layer associated to high Fe levels, while P was likely the ultimate
493 controlling factor of N-input by N₂-fixation in this region (Moutin et al., 2008; Moutin et al., 2018).
494 N₂-fixation rates were among the highest ever measured in the open ocean during OUTPACE in
495 this region (Bonnet et al., 2017), and the development of a mixed community, composed of
496 filamentous cyanobacteria such as *Trichodesmium* spp. and other spiraled-shaped species,
497 unicellular diazotrophs such as UCYN, *Crocospaera watsonii*, and Diatom-Diazotroph
498 Associations (DDAs) was observed (Appendix 3). The highest rates were measured at the surface
499 at stations 1, 5, 6 and LD-B (Caffin et al., this issue) and the major contributor to N₂-fixation in
500 MA waters was by far *Trichodesmium* (Bonnet et al., 2018). In the Niskin cell counts, DDAs known
501 to live in association with the diazotroph *Richelia intracellularis* such as *Hemiaulus hauckii*,
502 *Chaetoceros compressus* and several species of *Rhizosolenia* such as *R. styliformis*, *R. bergonii*, *R.*
503 *imbricata* and the centric *Climacodium frauenfeldianum* known to harbor a genus related to
504 *Cyanothece* sp. (Carpenter, 2002) were all found in low abundance in the water sample cell counts,
505 contributing to less than 1% of total diatoms. Exceptions were observed at sites 1 and 2 where their
506 contributions increased to 2.3 and 8% respectively. The low contribution of DDAs to the



507 diazotrophs community was confirmed by direct cell counts and *nifH* gene sequencing (Stenegren
508 et al., 2018). Notably, the presence of *Richelia intracellularis* was not observed in the Niskin lugol-
509 fixed water samples, but *Rhizosolenia styliformis* with *Richelia*, and some isolated *Richelia* cells
510 were observed abundantly in net hauls. The latter were found to be dominant at stations 1 and LD-
511 B, where the highest fixation rates were measured. *Richelia*, alone or in association with *R.*
512 *styliformis* were much less abundant in the South Pacific Gyre, where Fe is prone to be the limiting
513 nutrient for N₂-fixation rates despite higher P availability, pointing to less favorable growth
514 conditions for diazotrophs. Yet, the overall dominance of *Trichodesmium*, *Crocospaera* and other
515 filamentous cyanobacteria (Appendix 3) in the net samples reveals that DDAs were very minor
516 contributors to N₂-fixation during OUTPACE. This was also evidenced through NanoSIMS
517 analyses (Caffin et al., 2018). In order to explain the growth of diatoms in this severely N-depleted
518 region, one can quote the use of diazotroph-derived nitrogen (DDN), i.e. the secondary release of
519 N₂ fixed by diazotrophs, which showed to be efficiently channeled through the entire plankton
520 community during the VAHINE mesocosm experiment (Bonnet et al., 2016). In this latter study
521 off shore New Caledonia, *Cylindrotheca closterium* grew extensively after a stimulation of
522 diazotrophy after P-addition in large volume in situ mesocosms in New Caledonia (Leblanc et al.,
523 2016). As previous studies had already observed a co-occurrence of elevated *C. closterium* with
524 several diazotrophs (Devassy et al., 1978; Bonnet et al., 2016), this recurrent association tends to
525 confirm our previous hypothesis of a likely efficient use of DDN released as NH₄ by this fast
526 growing species (Leblanc et al., 2016). This could be another factor, besides Fe-availability,
527 explaining its success. A similar hypothesis may be invoked for the presence of *Mastogloia*
528 *woodiana*, a pennate diatom known to be occasionally dominant in the North Pacific Subtropical
529 Gyre blooms (Dore et al., 2008; Villareal et al., 2011). It is also a characteristic species of
530 oligotrophic areas (Guillard and Kilham, 1977), often observed in association with other DDAs,
531 which could similarly benefit from secondary N-release (Villareal et al., 2011; Krause et al., 2013).
532 Lastly, the ultra-oligotrophic region of the SPG investigated both during OUTPACE and BIOSOPE
533 revealed a base-line contribution of diatoms with often less than 200 cells L⁻¹ at the DCM and close
534 to zero at the surface. In addition, a dominance of small and large pennate species was observed,
535 such as *Nitzschia bicapitata*, *Pseudo-nitzschia delicatissima*, *Thalassiothrix longissima*,
536 *Thalassionema elegans* and *Pseudoeunotia* sp., that have already been documented for the
537 Equatorial Pacific by Guillard and Kilham (1977). Occasional occurrences of some emblematic



538 species of oligotrophic regions were also observed, such as *Chaetoceros dadayi*, *C. peruvianus*, *C.*
539 *tetrastichon* or *Planktoniella sol*. It can be noted that radiolarians were also more abundant and
540 more diverse in the ultra-oligotrophic SPG during OUTPACE than in the MA, while unfortunately
541 no information regarding radiolarians is available for the BIOSOPE cruise.

542 **5.3 Evidence for active Si uptake in the pico-planktonic size-fraction in the South Tropical** 543 **Pacific**

544 The pico-size fraction (<2-3 μm) represented on average 11% of BSi stocks during BIOSOPE, and
545 26% of BSi stocks during OUTPACE (Fig. 6), which is a non-negligible contribution. If the
546 importance of pico-size fraction in the BSi stock could be explained by detrital components, its
547 contribution to $\text{Si}(\text{OH})_4$ uptake during BIOSOPE was really surprising but could be explained in
548 the light of new findings. Indeed, recent studies have evidenced that the pico-phytoplanktonic
549 cyanobacteria *Synechococcus* can assimilate Si (Baines et al., 2012; Ohnemus et al., 2016; Krause
550 et al., 2017; Brzezinski et al., 2017), which could explain why Si stocks were detected in this size
551 fraction. The first hypothesis was to consider broken fragments of siliceous cells passing through
552 the filter or interferences with lithogenic silica, but these hypotheses were invalidated during
553 BIOSOPE when Si uptake measurements using ^{32}Si were also carried out on this pico-size fraction
554 and revealed a non-negligible uptake, mainly in the Chilean upwelling systems (Fig. 7). It is also
555 excluded that some broken parts of active nano-planktonic diatoms labelled with ^{32}Si could have
556 passed through the filters because of breakage during filtration, as a kinetic type response was
557 observed in most samples (Fig. 8), implying truly active organisms in the 0.2-2 μm size fraction.
558 Our results are thus in line with previous findings, as no other organisms below 2-3 μm are known
559 to assimilate Si, except some small size Parmales, a poorly described siliceous armored planktonic
560 group which span over the 2-10 μm size class, such as *Tetraparma* sp. (Ichinomiya, 2016), or small
561 nano-planktonic diatoms such as *Minidiscus* (Leblanc et al., 2018), close to the 2 μm limit (Fig. 11
562 a,b). The latter two species could occur in the 2-3 μm size-fraction, but are very easily missed in
563 light microscopy and require SEM imaging or molecular work for correct identification. Presence
564 of Parmales or nano-planktonic diatoms may explain the measurement of BSi in this 0.4 – 3 μm
565 size-class for the OUTPACE cruise, but can be excluded as responsible for the Si uptake measured
566 during BIOSOPE on filters below 2 μm . Rather, during OUTPACE, NanoSIMS imaging revealed
567 that cytometrically sorted *Synechococcus* cells accumulated Si (Fig. 11c), confirming their
568 potential role in the Si cycle in the South Tropical Gyre.



569 According to Baines et al. (2012), the Si content of *Synechococcus*, in some cases, could exceed
570 that of diatoms, but these authors suggested that they might exert a larger control on the Si cycle
571 in nutrient-poor waters where these organisms are dominant. In the present study, the largest
572 contribution of the pico-size fraction to absolute ΣpSi uptake rates occurred at both ends of the
573 transect in the Peru-Chile upwelling region and at the MAR station (Table 1), locations which also
574 corresponded to the highest concentrations of *Synechococcus* observed (Grob et al., 2007).
575 However, compared to diatoms, this only represented 1 to 5 % of total ΣpSi uptake, which is
576 probably not likely to drive the Si drawdown in this environment. This low relative contribution to
577 ΣpSi was similarly found at the other end of the transect at HNL and MAR station, but where
578 absolute uptake rates were moderate. The largest contribution of the pico-size fraction was
579 measured in the SPG (GYR and EGY sites), where despite very low pSi values, the relative ΣpSi
580 uptake between 0.2 and 2 μm reached 16 to 25 %. Station GYR as well as stations 13 to 15 are
581 areas that are highly depleted in orthosilicic acid, with concentrations $<1 \mu M$ from the surface to
582 as deep as 240 m. Hence, it is probable that *Synechococcus* could play a major role in depleting the
583 Si of surface waters in this area, which are devoid of diatoms. During the OUTPACE cruise, there
584 were no clear correlations between *Synechococcus* distributions and the measured 0.4-3 μm BSi
585 concentrations. This could be explained by the extremely wide range of individual cellular Si
586 quotas estimated to vary between 1 and 4700 $amol Si cell^{-1}$ (with an average value of 43) from cells
587 collected in the North Western Atlantic (Ohnemus et al., 2016), where *Synechococcus* contributed
588 up to 23.5 % of ΣBSi (Krause et al., 2017). In the latter study, a first-order estimate of the
589 contribution of *Synechococcus* to the global annual Si production flux amounted to 0.7-3.5%,
590 which is certainly low, but comparable to some other important input or output fluxes of Si (Tréguer
591 and De la Rocha, 2013).

592 **6 Conclusion**

593 The Sargasso Sea (BATS) and the North Tropical Pacific Ocean (ALOHA) were until now the
594 only two subtropical gyres where the Si cycle was fully investigated during time-series surveys. In
595 this paper, we provide the first complementary data from two cruises documenting production,
596 biomass and export fluxes from the oligotrophic to ultra-oligotrophic conditions in the South
597 Tropical Pacific Gyre, which may lower the estimates of diatom contribution to primary



598 productivity and export fluxes for the Pacific Ocean and for mid-ocean gyres in general. The mid-
599 ocean gyres (representing 1/3 of the global ocean) are severely under-sampled regarding the Si
600 cycle, and may encompass very different situations, in particular in the vicinity of Islands and
601 archipelagos with reduced bathymetry, and nutrient-fertilized surface waters, to HNLC waters and
602 even HNLSiLC along the equatorial divergence (Dugdale and Wilkerson, 1998). The mid-ocean
603 gyres contribution to Si production was recently revised down to 5-7% of the total by Brzezinski
604 et al. (2011) building on estimates from the North Subtropical Pacific Gyre. The present study
605 points to even lower values for the South Pacific Gyre, confirming its ultra-oligotrophic nature,
606 and should further decrease this estimate. These findings clearly warrant for improved coverage of
607 these areas and for more complete elemental studies (from Si production to export).

608 Diatom community structure and contribution to total biomass could be summarized by
609 differentiating 3 main ecosystems: (i) the eutrophic Peru-Chile coastal upwelling, where colonial
610 neritic centric diatoms such as *Skeletonema* sp., *Chaetoceros* sp. and *Thalassiosira* sp. contributed
611 to elevated abundances ($>100,000$ cells L^{-1}) and very high Si uptake rates; (ii) the HNLC region
612 off the Marquesas Islands and the nutrient depleted but Fe-fertilized region of the Melanesian
613 Archipelago, where a distinct community largely dominated by small and medium-sized pennates
614 such as *Cylindrotheca closterium* and *Pseudo-nitzschia delicatissima* developed to moderate levels
615 ($<30,000$ cells L^{-1}), while Fe levels in the MA further stimulated diazotrophs and DDAs which
616 could have stimulated diatom growth through secondary N release; (iii) the SPG, characterized by
617 ultra-oligotrophic conditions and Fe-limitation, where diatoms reached negligible abundances
618 (<200 cells L^{-1}) with species typical of oligotrophic regions, such as *Nitzschia bicaipitata*,
619 *Mastogloia woodiana*, *Planktoniella sol* as well as radiolarians.

620 Finally, thanks to both size-fractionated biomass and Si uptake measurements, we were able to
621 confirm a potential role for *Synechococcus* cells in Si uptake in all environments, which may be of
622 importance relative to diatoms in oligotrophic regions, but probably negligible in highly productive
623 regions such as coastal upwellings. Mechanisms linked to Si uptake in *Synechococcus* and its
624 ecological function still need to be elucidated, and further attention to the Si cycle needs to be
625 placed on this elusive pico- and nano-sized fraction.



626 **7 Data availability**

627 **8 Author contribution**

628 KL treated all data and wrote the paper. BQ and PR sampled on board and analyzed Si data from
629 the BIOSOPE cruise. SH-N and O.G. collected nutrient samples on board and analyzed nutrient
630 data from the OUTPACE cruise. VC sampled for all BSi data and diatom diversity on board, and
631 analyzed plankton net samples on the OUTPACE cruise. CB analyzed all Si data and ran diatom
632 cell counts during her Masters thesis. HC and JR were in charge of all pigment data for both cruises.
633 NL collected and analyzed Si export flux data from the OUTPACE drifting sediment traps.

634 **9 Competing interests**

635 The authors declare that they have no conflict of interest.

636 **10 Special Issue Statement**

637 This article is part of the special issue “Interactions between planktonic organisms and
638 biogeochemical cycles across trophic and N₂ fixation gradients in the western tropical South Pacific
639 Ocean: a multidisciplinary approach (OUTPACE experiment)”

640 **11 Acknowledgments**

641 This work is part of the OUTPACE Experiment project (<https://outpace.mio.univ-amu.fr/>) funded
642 by the Agence Nationale de la Recherche (grant ANR-14-CE01-0007-01), the LEFE-CyBER
643 program (CNRS-INSU), the Institut de Recherche pour le Développement (IRD), the GOPS
644 program (IRD) and the CNES (BC T23, ZBC 4500048836), and the European FEDER Fund under
645 project 1166-39417). The OUTPACE cruise (<http://dx.doi.org/10.17600/15000900>) was managed
646 by the MIO (OSU Institut Pytheas, AMU) from Marseilles (France). The BIOSOPE project was
647 funded by the Centre National de la Recherche Scientifique (CNRS), the Institut des Sciences de
648 l’Univers (INSU), the Centre National d’Etudes Spatiales (CNES), the European Space Agency
649 (ESA), The National Aeronautics and Space Administration (NASA) and the Natural Sciences and
650 Engineering Research Council of Canada (NSERC). This is a contribution to the BIOSOPE project
651 of the LEFE-CYBER program. The project leading to this publication has received funding from



652 European FEDER Fund under project 1166-39417. We warmly thank the captain, crew and CTD
653 operators on board R/V I'Atalante during both cruises. We further acknowledge Fernando Gomez
654 for providing diatom cell counts during BIOSOPE, Dr Jeremy Young at University College of
655 London for allowing the use of Parmale image from the Nannotax website and Mathieu Caffin for
656 providing a NanoSIMS image of *Synechococcus* collected during OUTPACE showing cellular Si
657 accumulation.
658

659 12 References

- 660 Adjou, M., Tréguer, P. J., Dumousseaud, C., Corvaisier, R., Brzezinski, M. A., and Nelson, D. M.: Particulate silica
661 and Si recycling in the surface waters of the Eastern Equatorial Pacific, Deep-Sea Research Part II: Topical Studies in
662 Oceanography, 58, 449-461, 2011.
- 663 Aminot, A. and Kérouel, R.: Dosage automatique des nutriments dans les eaux marines: méthodes en flux continu,
664 Editions Quae, 2007.
- 665 Assmy, P., Henjes, J., Klaas, C., and Smetacek, V. S.: Mechanisms determining species dominance in a phytoplankton
666 bloom induced by the iron fertilization experiment EisenEx in the Southern Ocean, Deep-Sea Research Part I:
667 Oceanographic Research Papers, 54, 340-362, 2007.
- 668 Avaria, S. and Munoz, P.: Effects of the 1982-1983 El Nino on the marine phytoplankton off Northern Chile, Journal
669 of Geophysical Research, 92, 14,369-314,382, 1987.
- 670 Baines, S. B., Twining, B. S., Brzezinski, M. A., Krause, J. W., Vogt, S., Assael, D., and McDaniel, H.: Significant
671 silicon accumulation by marine picocyanobacteria, Nature Geoscience, 5, 886-891, 2012.
- 672 Blain, S., Bonnet, S., and Guieu, C.: Dissolved iron distribution in the tropical and sub tropical South Eastern Pacific,
673 Biogeosciences, 5, 269-280, 2008.
- 674 Blain, S., Leynaert, A., Tréguer, P. J., Chrétiennot-Dinet, M.-J., and Rodier, M.: Biomass, growth rates and limitation
675 of Equatorial Pacific diatoms, Deep Sea Research Part I: Oceanographic Research Papers, 44, 1255-1275, 1997.
- 676 Bonnet, S., Berthelot, H., Turk-Kubo, K., Cornet-Barthaux, V., Fawcett, S., Berman-Frank, I., Barani, A., Grégori, G.,
677 Dekaezemacker, J., Benavides, M., and Capone, D. G.: Diazotroph derived nitrogen supports diatom growth in the
678 South West Pacific: A quantitative study using nanoSIMS, Limnology and Oceanography, 61, 1549-1562, 2016.
- 679 Bonnet, S., Caffin, M., Berthelot, H., and Moutin, T.: Hot spot of N₂ fixation in the western tropical South Pacific
680 pleads for a spatial decoupling between N₂ fixation and denitrification, Proceedings of the National Academy of
681 Sciences, 114, E2800-E2801, 2017.
- 682 Bonnet, S., Caffin, M., Berthelot, H., Grosso, O., Benavides, M., Hélias-Nunige, S., Guieu, C., Stenegren, M and
683 Foster, R. A.: In depth characterization of diazotroph activity across the Western Tropical South Pacific hot spot of N₂
684 fixation, Biogeosciences Discuss., 2018, 1 – 30, doi:10.5194/bg-2017-567, 2018.
- 685 Brzezinski, M. A., Dumousseaud, C., Krause, J. W., Measures, C. I., and Nelson, D. M.: Iron and silicic acid
686 concentrations together regulate Si uptake in the equatorial Pacific Ocean, Limnology and Oceanography, 53, 875-
687 889, 2008.



- 688 Brzezinski, M. A. and Kosman, C. A.: Silica production in the Sargasso Sea during spring 1989, *Marine Ecology*
689 *Progress Series*, 142, 39-45, 1996.
- 690 Brzezinski, M. A., Krause, J. W., Baines, S. B., Collier, J. L., Ohnemus, D. C., and Twining, B. S.: Patterns and
691 regulation of silicon accumulation in *Synechococcus* spp., *Journal of Phycology*, 53, 746-761, 2017.
- 692 Brzezinski, M. A., Krause, J. W., Church, M. J., Karl, D. M., Li, B., Jones, J. L., and Updyke, B.: The annual silica
693 cycle of the North Pacific subtropical gyre, *Deep-Sea Research Part I: Oceanographic Research Papers*, 58, 988-1001,
694 2011.
- 695 Brzezinski, M. A. and Nelson, D. M.: The annual silica cycle in the Sargasso Sea near Bermuda, *Deep-Sea Research*
696 *Part I*, 42, 1215-1237, 1995.
- 697 Brzezinski, M. A. and Nelson, D. M.: Seasonal changes in the silicon cycle within a Gulf Stream warm-core ring, *Deep*
698 *Sea Research Part A. Oceanographic Research Papers*, 36, 1009-1030, 1989.
- 699 Brzezinski, M. A., Phillips, D. R., Chavez, F. P., Friederich, G. E., and Dugdale, R. C.: Silica production in the
700 Monterey, California, upwelling system, *Limnology and Oceanography*, 42, 1694-1705, 1997.
- 701 Brzezinski, M. A., Villareal, T. A., and Lipschultz, F. F.: Silica production and the contribution of diatoms to new and
702 primary production in the central North Pacific, *Marine Ecology-Progress Series*, 167, 89-104, 1998.
- 703 Buck, K. R. and Chavez, F. P.: Diatom aggregates from the open ocean, *Journal of Plankton Research*, 16, 1449-1457,
704 1994.
- 705 Caffin, M., Berthelot, H., Cornet-Barthaux, V., and Bonnet, S.: Transfer of diazotroph-derived nitrogen to the
706 planktonic food web across gradients of N₂ fixation activity and diversity in the Western Tropical South Pacific,
707 *Biogeosciences Discuss.*, 2018, 1-32, 2018.
- 708 Carlotti, F., Pagano, M., Guilloux, L., Donoso, K., Valdés, V., and Hunt, B. P. V.: Mesozooplankton structure and
709 functioning in the western tropical South Pacific along the 20° parallel south during the OUTPACE survey (February-
710 April 2015), *Biogeosciences Discuss.*, 2018, 1-51, 2018.
- 711 Carpenter, E. J.: *Marine Cyanobacterial Symbioses*, 102B, 15-18, 2002.
- 712 Chavez, F. P., Buck, K. R., and Barber, R. T.: Phytoplankton taxa in relation to primary production in the equatorial
713 Pacific, *Deep Sea Research Part A. Oceanographic Research Papers*, 37, 1733-1752, 1990.
- 714 Chavez, F. P., Buck, K. R., Coale, K. H., Martin, J. H., DiTullio, G. R., Welschmeyer, N. A., Jacobson, A. C., and
715 Barber, R. T.: Growth rates, grazing, sinking, and iron limitation of equatorial Pacific phytoplankton, *Limnology and*
716 *Oceanography*, 36, 1816-1833, 1991.
- 717 Chavez, F. P., Buck, K. R., Service, S. K., Newton, J., and Barber, R. T.: Phytoplankton variability in the central and
718 eastern tropical Pacific, *Deep-Sea Research Part II-Topical Studies in Oceanography*, 43, 835-+, 1996.
- 719 Chisholm, S. W.: *Phytoplankton Size*, doi: 10.1007/978-1-4899-0762-2_12, 1992. 213-237, 1992.
- 720 Claustre, H., Sciandra, A., and Vault, D.: Introduction to the special section bio-optical and biogeochemical
721 conditions in the South East Pacific in late 2004: The BIOSOPE program, *Biogeosciences*, 5, 679-691, 2008.
- 722 Crombet, Y., Leblanc, K., Quéguiner, B., Moutin, T., Rimmelin, P., Ras, J., Claustre, H., Leblond, N., Oriol, L., and
723 Pujo-Pay, M.: Deep silicon maxima in the stratified oligotrophic Mediterranean Sea, *Biogeosciences*, 8, 459-475, 2011.



- 724 de Verneil, A., Rousselet, L., Doglioli, A. M., Petrenko, A. A., Maes, C., Bouruet-Aubertot, P., and Moutin, T.:
725 OUTPACE long duration stations: physical variability, context of biogeochemical sampling, and evaluation of
726 sampling strategy, *Biogeosciences*, 15, 2125-2147, 2018.
- 727 Demarest, M. S., Brzezinski, M. A., Nelson, D. M., Krause, J. W., Jones, J. L., and Beucher, C. P.: Net biogenic silica
728 production and nitrate regeneration determine the strength of the silica pump in the Eastern Equatorial Pacific, *Deep-
729 Sea Research Part II: Topical Studies in Oceanography*, 58, 462-476, 2011.
- 730 Devassy, V. P., Bhattathiri, P. M. A., and Qasim, S. Z.: Trichodesmium phenomenon, *Indian J. Mar. Sci.*, 7, 168-186,
731 1978.
- 732 Dore, J. E., Letelier, R. M., Church, M. J., Lukas, R., and Karl, D. M.: Summer phytoplankton blooms in the
733 oligotrophic North Pacific Subtropical Gyre: Historical perspective and recent observations, *Progress in
734 Oceanography*, 76, 2-38, 2008.
- 735 Dugdale, R. C. and Wilkerson, F. P.: Silicate regulation of new production in the equatorial Pacific upwelling, *Nature*,
736 391, 270-273, 1998.
- 737 Fryxell, G. A. and Kaczmarek, I.: Specific variability in Fe-enriched cultures from the equatorial Pacific, *Journal of
738 plankton research*, 16, 755-769, 1994.
- 739 Fumenia, A., Moutin, T., Bonnet, S., Benavides, M., Petrenko, A., Helias Nunige, S., and Maes, C.: Excess nitrogen
740 as a marker of intense dinitrogen fixation in the Western Tropical South Pacific Ocean: impact on the thermocline
741 waters of the South Pacific, *Biogeosciences Discuss.*, 2018, 1-33, 2018.
- 742 Gomez, F., Claustre, H., Raimbault, P., and Souissi, S.: Two High-Nutrient Low-Chlorophyll phytoplankton
743 assemblages: the tropical central Pacific and the offshore Peru -Chile Current, *Biogeosciences*, 4, 1101-1113, 2007.
- 744 Grob, C., Ulloa, O., Claustre, H., Huot, Y., Alarcn, G., and Marie, D.: Contribution of picoplankton to the total
745 particulate organic carbon concentration in the eastern South Pacific, *Biogeosciences*, 4, 837-852, 2007.
- 746 Guieu, C., Bonnet, S., Petrenko, A., Menkes, C., Chavagnac, V., Desboeufs, K., and Moutin, T.: Iron from a submarine
747 source impacts the productive layer of the Western Tropical South Pacific (WTSP), *Nature Sci. Rep.*, in rev. in rev.
- 748 Guillard, R. R. L. and Kilham, P.: The ecology of marine planktonic diatoms, 13, 372-469, 1977.
- 749 Hasle, G. R.: Phytoplankton and ciliate species from the tropical Pacific, 1960. 1960.
- 750 Honjo, S. and Manganini, S. J.: Annual biogenic particle fluxes to the interior of the North Atlantic Ocean; studied at
751 34°N 21°W and 48°N 21°W, *Deep-Sea Research Part II*, 40, 587-607, 1993.
- 752 Ichinomiya, M. a.: Diversity and oceanic distribution of the Parmales (Bolidophyceae), a picoplanktonic group closely
753 related to diatoms, *ISME Journal*, 10, 2419-2434, 2016.
- 754 Iriarte, J. L. and Fryxell, G. A.: Micro-phytoplankton at the equatorial Pacific (140°W) during the JGOFS EqPac Time
755 Series studies: March to April and October 1992, *Deep-Sea Research Part II*, 42, 559-583, 1995.
- 756 Jimenez, R.: Composition and distribution of phytoplankton in the upwelling system of the Galapagos Islands, *Coastal
757 and Estuarine Sciences*, 1, 39-43, 1981.
- 758 Kaczmarek, I. and Fryxell, G. A.: Micro-phytoplankton of the equatorial Pacific: 140°W meridional transect during
759 the 1992 El Nino, *Deep-Sea Research Part II*, 42, 535-558, 1995.



- 760 Kobayashi, F. and Takahashi, K.: Distribution of diatoms along the equatorial transect in the western and central Pacific
761 during the 1999 La Nina conditions, *Deep-Sea Research Part II: Topical Studies in Oceanography*, 49, 2801-2821,
762 2002.
- 763 Krause, J. W., Brzezinski, M. A., Baines, S. B., Collier, J. L., Twining, B. S., and Ohnemus, D. C.: Picoplankton
764 contribution to biogenic silica stocks and production rates in the Sargasso Sea, *Global Biogeochemical Cycles*,
765 Accepted, 1-13, 2017.
- 766 Krause, J. W., Brzezinski, M. A., Goericke, R., Landry, M. R., Ohman, M. D., Stukel, M. R., and Taylor, A. G.:
767 Variability in diatom contributions to biomass, organic matter production and export across a frontal gradient in the
768 California Current Ecosystem, *Journal of Geophysical Research: Oceans*, 120, 1032-1047, 2015.
- 769 Krause, J. W., Brzezinski, M. A., Villareal, T. A., and Wilson, C.: Biogenic silica cycling during summer
770 phytoplankton blooms in the North Pacific subtropical gyre, *Deep-Sea Research Part I: Oceanographic Research
771 Papers*, 71, 49-60, 2013.
- 772 Krause, J. W., Nelson, D. M., and Brzezinski, M. A.: Biogenic silica production and the diatom contribution to primary
773 production and nitrate uptake in the eastern equatorial Pacific Ocean, *Deep-Sea Research Part II: Topical Studies in
774 Oceanography*, 58, 434-448, 2011.
- 775 Krause, J. W., Nelson, D. M., and Lomas, M. W.: Biogeochemical responses to late-winter storms in the Sargasso Sea,
776 II: Increased rates of biogenic silica production and export, *Deep-Sea Research Part I: Oceanographic Research Papers*,
777 56, 861-874, 2009.
- 778 Krause, J. W., Nelson, D. M., and Lomas, M. W.: Production, dissolution, accumulation, and potential export of
779 biogenic silica in a Sargasso Sea mode-water eddy, *Limnology and Oceanography*, 55, 569-579, 2010.
- 780 Leblanc, K., Cornet, V., Caffin, M., Rodier, M., Desnues, A., Berthelot, H., Turk-Kubo, K., and Heliou, J.:
781 Phytoplankton community structure in the VAHINE mesocosm experiment, *Biogeosciences*, 13, 5205-5219, 2016.
- 782 Leblanc, K., Hare, C. E., Boyd, P. W., Bruland, K. W., Sohst, B., Pickmere, S., Lohan, M. C., Buck, K. N., Ellwood,
783 M. J., and Hutchins, D. A.: Fe and Zn effects on the Si cycle and diatom community structure in two contrasting high
784 and low-silicate HNLC areas, *Deep-Sea Research Part I: Oceanographic Research Papers*, 52, 1842-1864, 2005a.
- 785 Leblanc, K., Leynaert, A., Fernandez, C. I., Rimmelin, P., Moutin, P., Raimbault, P., Ras, J., and Quéguiner, B.: A
786 seasonal study of diatom dynamics in the North Atlantic during the POMME experiment (2001): Evidence for Si
787 limitation of the spring bloom, *Journal of Geophysical Research*, 110, C07S14, 2005b.
- 788 Leblanc, K., Quéguiner, B., Diaz, F., Cornet, V., Michel-Rodriguez, M., Durrieu de Madron, X., Bowler, C., Malviya,
789 S., Thyssen, M., Grégori, G., Rembauville, M., Grosso, O., Poulain, J., de Vargas, C., Pujo-Pay, M., and Conan, P.:
790 Nanoplanktonic diatoms are globally overlooked but play a role in spring blooms and carbon export, *Nature
791 Communications*, 9, 953, 2018.
- 792 Leblanc, K., Quéguiner, B., Garcia, N., Rimmelin, P., and Raimbault, P.: Silicon cycle in the NW Mediterranean Sea:
793 Seasonal study of a coastal oligotrophic site, *Oceanologica Acta*, 26, 339-355, 2003.
- 794 Leynaert, A.: La production de silice biogénique dans l'océan : de la mer de Weddell à l'océan Antarctique., 1993. 99,
795 1993.
- 796 Leynaert, A., Trguer, P. J., Lancelot, C., and Rodier, M.: Silicon limitation of biogenic silica production in the
797 Equatorial Pacific, *Deep-Sea Research Part I: Oceanographic Research Papers*, 48, 639-660, 2001.
- 798 Mosseri, J., Quéguiner, B., Rimmelin, P., Leblond, N., and Guieu, C.: Silica fluxes in the northeast Atlantic frontal
799 zone of Mode Water formation (38–45 N, 16–22 W) in 2001–2002, *Journal of Geophysical Research: Oceans*, 110,
800 2005.



- 801 Moutin, T., Karl, D. M., Duhamel, S., Rimmelin, P., Raimbault, P., Van Mooy, B. A. S., and Claustre, H.: Phosphate
802 availability and the ultimate control of new nitrogen input by nitrogen fixation in the tropical Pacific Ocean,
803 *Biogeosciences*, 5, 95-109, 2008.
- 804 Moutin, T., Doglioli, A. M., de Verneil, A., and Bonnet, S.: Preface: The Oligotrophy to the Ultra-oligotrophy PACific
805 Experiment (OUTPACE cruise, 18 February to 3 April 2015), *Biogeosciences*, 14, 3207-3220, 2017.
- 806 Moutin, T., Wagener, T., Caffin, M., Fumenia, A., Gimenez, A., Baklouti, M., Bouruet-Aubertot, P., Pujo-Pay, M.,
807 Leblanc, K., Lefevre, D., Helias Nunige, S., Leblond, N., Grosso, O., and de Verneil, A.: Nutrient availability and the
808 ultimate control of the biological carbon pump in the Western Tropical South Pacific Ocean, *Biogeosciences Discuss.*,
809 2018, 1-41, 2018.
- 810 Nelson, D., Goering, J., and Boisseau, D.: Consumption and regeneration of silicic acid in three coastal upwelling
811 systems, *Coastal upwelling*, 1981. 242-256, 1981.
- 812 Nelson, D. M. and Brzezinski, M. A.: Diatom growth and productivity in an oligo-trophic midocean gyre: A 3-yr
813 record from the Sargasso Sea near Bermuda, *Limnology and Oceanography*, 42, 473-486, 1997.
- 814 Nelson, D. M. and Goering, J. J.: Assimilation of silicic acid by phytoplankton in the Baja California and northwest
815 Africa upwelling systems, *Limnology and Oceanography*, 23, 508-517, 1978.
- 816 Nelson, D. M., Smith, W. O., Muench, R. D., Gordon, L. I., Sullivan, C. W., and Husby, D. M.: Particulate matter and
817 nutrient distributions in the ice-edge zone of the Weddell Sea: relationship to hydrography during late summer, *Deep
818 Sea Research Part A. Oceanographic Research Papers*, 36, 191-209, 1989.
- 819 Nelson, D. M., Tréguer, P. J., Brzezinski, M. A., Leynaert, A., and Quéguiner, B.: Production and dissolution of
820 biogenic silica in the ocean: Revised global estimates, comparison with regional data and relationship to biogenic
821 sedimentation, *Global Biogeochemical Cycles*, 9, 359-372, 1995.
- 822 Ohnemus, D. C., Rauschenberg, S., Krause, J. W., Brzezinski, M. A., Collier, J. L., Geraci-Yee, S., Baines, S. B., and
823 Twining, B. S.: Silicon content of individual cells of *Synechococcus* from the North Atlantic Ocean, *Marine Chemistry*,
824 187, 16-24, 2016.
- 825 Paasche, E.: Silicon and the ecology of marine plankton diatoms. I. *Thalassiosira pseudonana* (*Cyclotella nana*) grown
826 in a chemostat with silicate as limiting nutrient., *Marine Biology*, 19, 117-126, 1973.
- 827 Quéguiner, B.: Iron fertilization and the structure of planktonic communities in high nutrient regions of the Southern
828 Ocean, *Deep Sea Research Part II: Topical Studies in Oceanography*, 90, 43-54, 2013.
- 829 Ragueneau, O. and Tréguer, P. J.: Determination of biogenic silica in coastal waters: applicability and limits of the
830 alkaline digestion method, *Marine Chemistry*, 45, 43-51, 1994.
- 831 Ragueneau, O., Tréguer, P. J., Leynaert, A., Anderson, R. F., Brzezinski, M. A., DeMaster, D. J., Dugdale, R. C.,
832 Dymond, J., Fischer, G., Francois, R., Heinze, C., Maier-Reimer, E., Martin-Jézéquel, V., Nelson, D. M., and
833 Quéguiner, B.: A review of the Si cycle in the modern ocean: recent progress and missing gaps in the application of
834 biogenic opal as a paleoproductivity proxy, *Global and Planetary Change*, 26, 317-365, 2000.
- 835 Raimbault, P., Garcia, N., and Cerutti, F.: Distribution of inorganic and organic nutrients in the South Pacific Ocean
836 − evidence for long-term accumulation of organic matter in nitrogen-depleted waters, *Biogeosciences*, 5, 281-
837 298, 2008.
- 838 Ras, J., Claustre, H., and Uitz, J.: Spatial variability of phytoplankton pigment distributions in the Subtropical South
839 Pacific Ocean: comparison between in situ and predicted data, *Biogeosciences Discussions*, 4, 3409-3451, 2008.



- 840 Rivera, P., Herrera, L., and Barrales, H.: Report of two species of *Thalassiosira* (Bacillariophyceae): *T. rotula* Meunier
841 and *T. anguste-lineata* (A. Schmidt) Fryxell et Hasle, as new to northern Chile, *Cryptogamie. Algologie*, 17, 123-130,
842 1996.
- 843 Semina, H. J. and Levashova, S. S.: the Biogeography of Tropical Phytoplankton Species in the Pacific-Ocean,
844 *Internationale Revue Der Gesamten Hydrobiologie*, 78, 243-262, 1993.
- 845 Stenegren, M., Caputo, A., Berg, C., Bonnet, S., and Foster, R. A.: Distribution and drivers of symbiotic and free-
846 living diazotrophic cyanobacteria in the western tropical South Pacific, *Biogeosciences*, 15, 1559-1578, 2018.
- 847 Strickland, J. D. H. and Parsons, T. R.: A practical handbook of seawater analysis, Fisheries Research Board of Canada
848 Bulletin, 167, 310, 1972.
- 849 Tréguer, P. J. and De la Rocha, C. L.: The world ocean silica cycle., *Annual review of marine science*, 5, 477-501,
850 2013.
- 851 Tréguer, P. J. and Lindner, L.: Production of biogenic silica in the Weddell-Scotia Seas measured with ^{32}Si , *Limnology*
852 and *Oceanography*, 36, 1217-1227, 1991.
- 853 Villareal, T. A., Adornato, L., Wilson, C., and Schoenbaechler, C. A.: Summer blooms of diatom-diazotroph
854 assemblages and surface chlorophyll in the North Pacific gyre: A disconnect, *Journal of Geophysical Research*, 116,
855 C03001, 2011.
- 856 Wilson, C.: Chlorophyll anomalies along the critical latitude at 30N in the NE Pacific, *Geophysical Research Letters*,
857 38, 1-6, 2011.
- 858 Wilson, C.: Late summer chlorophyll blooms in the oligotrophic North Pacific Subtropical Gyre, *Geophysical*
859 *Research Letters*, 30, 4-7, 2003.
- 860 Wong, C. S. and Matear, R. J.: Sporadic silicate limitation of phytoplankton productivity in the subarctic NE Pacific,
861 *Deep-Sea Research Part II: Topical Studies in Oceanography*, 46, 2539-2555, 1999.
862
- 863
- 864
- 865
- 866
- 867



868 13 Figure Legend

869 **Figure 1:** Bathymetric map of the stations sampled in the South Pacific Ocean during the OUTPACE cruise (Feb.-Apr. 2015) and
870 the BIOSOPE cruise (Oct.-Nov. 2004). Short-term duration stations are indicated in white, and long-term duration stations (typically
871 2-3d) in black.

872 **Figure 2:** Nutrient distribution (orthosilicic acid, nitrate, phosphate, in μM) along the OUTPACE cruise transect.

873 **Figure 3:** Nutrient distribution (orthosilicic acid, nitrate, phosphate, in μM) along the BIOSOPE cruise transect.

874 **Figure 4 :** Top panel: TChla distribution during the OUTPACE cruise in the SW Pacific (in $\mu\text{g L}^{-1}$) with fucoxanthin overlay lines
875 in white (in ng L^{-1}). Lower panel: TChla distribution during the BIOSOPE cruise in the SW Pacific (in $\mu\text{g L}^{-1}$) with fucoxanthin
876 overlay lines in white (in ng L^{-1}). Black dots indicated the Ze depth.

877 **Figure 5:** a.c Biogenic silica (BSi) and b.d. Lithogenic Silica (LSi) distribution during the OUTPACE and BIOSOPE cruises
878 respectively (in $\mu\text{mol L}^{-1}$).

879 **Figure 6:** a.b Size-fractionated integrated Biogenic silica (Σ BSi) standing stocks (0-125 m) during the BIOSOPE cruise. UPW1
880 stations was only integrated over 50 m and UPX1 and UPX2 over 100 m. The b panel shows a zoom over the central section where
881 integrated BSi stocks are an order of magnitude lower than at the two extremities of the transect. Grey bars indicate that no size-
882 fractionation was conducted and represent the total Σ BSi. C. Size-fractionated integrated Biogenic silica (Σ BSi) standing stocks
883 (0-125 m) during the OUTPACE cruise.

884 **Figure 7:** a. Total absolute Si uptake rates (ρSi) vertical profiles (in $\mu\text{mol L}^{-1} \text{d}^{-1}$) at the LD stations MAR, HNL, GYR, EGY,
885 UPX and UPW. b. ρSi in the 0.2 - 2 μm size fraction at the same sites.

886 **Figure 8:** Si uptake kinetic experiments conducted at the LD stations MAR, HNL, GYR, EGY, UPX at various euphotic depths.
887 Specific Si uptake rates (in d^{-1}) are plotted vs $\text{Si}(\text{OH})_4$ increasing concentrations. Data was adjusted with hyperbolic curves when
888 statistically relevant and V_{max} and K_s values indicated below each curve.

889 **Figure 9:** Diatoms cellular concentrations (cells L^{-1}) derived from a. Niskin cell counts, b. number of taxa and c. relative contribution
890 to POC biomass (%) at the surface and DCM levels during the OUTPACE cruise.

891 **Figure 10:** Diatoms cellular concentrations (cells L^{-1}) derived from Niskin cell counts at several depths during the BIOSOPE cruise
892 (data from Gomez et al. 2007).

893 **Figure 11:** Potential siliceous organisms in the picoplanktonic (<2-3 μm) size fraction. a.Siliceous scale-bearing Parmale
894 (*Tetraparma pelagica* in SEM, photo courtesy of Dr. J. Young), b. centric diatom (*Minidiscus trioculatus*), c. *Synechococcus* cell
895 showing Si assimilation in red (^{28}Si) in NanoSIMS (photo courtesy of M. Caffin).

896

897

898

899

900 **14 Tables**

901 **Table 1: Size-fractionated integrated Si production rates in mmol Si m⁻² d⁻¹ in the SEP (BIOSOPE). Integrated Si production**
 902 **was measured over the 0-1% light depth range for each site (in parenthesis in column 5), and normalized over 100 m**
 903 **considering a zero production at 100 m in the last column.**

Stations	$\Sigma\rho\text{Si} < 2\mu\text{m}$	$\Sigma\rho\text{Si} 2-10\mu\text{m}$	$\Sigma\rho\text{Si} > 10\mu\text{m}$	Total $\Sigma\rho\text{Si}$	Total $\Sigma\rho\text{Si}$ over 0-100 m
MAR1	0.15	0.51	4.37	5.02 (50 m)	5.87
HNL1	0.05	0.12	0.58	0.75 (80 m)	0.77
GYR2	0.01	0.01	0.02	0.04 (110 m)	0.04
EGY	0.03	0.07	0.09	0.19 (100 m)	0.19
UPW2	0.62	2.88	39.66	43.16 (35 m)	52.36
UPX1	1.07	5.90	13.49	20.46 (30 m)	42.46

904

905 **Table 2: Dominant diatom species in each main system of the BIOSOPE and OUTPACE cruises. Taxonomic information**
 906 **for the OUTPACE cruise are derived from discrete samplings at the surface and DCM and phytoplankton nets, while**
 907 **information for the BIOSOPE cruise were obtained through an average of six discrete samples over the euphotic layer (see**
 908 **Gomez et al., 2007).**

Cruise	Oceanic system	Dominant diatom species
OUTPACE	Melanesian Archipelago	<i>Pseudo-nitzschia</i> spp. & <i>Pseudo-nitzschia delicatissima</i> , <i>Cylindrotheca closterium</i> , <i>Mastogloia woodiana</i> , <i>Leptocylindrus mediterraneus</i> , <i>Hemiaulus membranaceus</i> , <i>Chaetoceros</i> spp. (<i>hyalochaete</i>), <i>Pseudosolenia calcar-</i> <i>avis</i> , <i>Climacodium frauenfeldianum</i> , <i>Planktoniella sol</i>
	South Pacific Gyre	<i>Climacodium frauenfeldianum</i> , <i>Pseudo-nitzschia</i> spp., <i>Chaetoceros</i> spp. (<i>hyalochaete</i>), <i>Pseudo-nitzschia</i> <i>delicatissima</i> , <i>Mastogloia woodiana</i>
BIOSOPE	Western HNLC area (Marquesas)	<i>Pseudo-nitzschia delicatissima</i> , <i>Rhizosolenia bergonii</i> , <i>Thalassiothrix longissima</i> , <i>Plagiotropis</i> spp., <i>Pseudo-</i> <i>nitzschia pungens</i> , <i>P. subpacific</i>
	South Tropical Pacific	<i>Nitzschia bicapitata</i> species complex, <i>Nitzschia</i> sp., <i>Thalassiothrix longissima</i> , <i>Pseudo-nitzschia delicatissima</i>
	South Pacific Gyre	<i>Hemiaulus hauckii</i> , <i>Chaetoceros curvisetus</i> , <i>Bacteriastrum</i> <i>cf. comosum</i>
	Eastern Gyre	<i>Pseudo-nitzschia</i> cf. <i>delicatissima</i> , <i>Pseudo-nitzschia</i> cf. <i>subpacific</i> , <i>Pseudoeunotia</i> sp.
	Peru-Chile Upwelling	<i>Chaetoceros compressus</i> , <i>Bacteriastrum</i> sp., <i>Thalassiosira</i> <i>subtilis</i> , <i>Chaetoceros</i> cf. <i>diadema</i> , <i>Skeletonema</i> sp., <i>Pseudo-nitzschia</i> sp.

909

910

911

912



913 **Table 3: Particulate biogenic and lithogenic (BSi and LSi) Silica in drifting sediment traps at each long duration station**
 914 **during OUTPACE cruise, at 153, 328 and 519 m depth.**

915

916

917

918

919

920

921

922

923

924 **Table 4: Integrated Si production rates in various systems for comparison with our study from direct ³²Si uptake**
 925 **measurements or from indirect silicate utilization (Δ SiO₄) estimates (*).**

Region	Integrated Si production rate Σ pSi (mmol m ⁻² d ⁻¹)	References
Coastal upwellings		
BIO SOPE: Peru-Chile upwelling	42 – 52 (UPW)	<i>This study</i>
Baja California	89	Nelson and Goering, 1978
Monterey Bay	70	Brzezinski et al., 1997
Peru	27	Nelson et al., 1981
Southern California Current coastal waters	1.7 – 5.6	Krause et al., 2015
Oceanic area		
BIO SOPE: South Eastern Pacific (HNLC)	0.8 – 5.6 (HNL – MAR)	<i>This study</i>
Gulf Stream warm rings	6.4	Brzezinski and Nelson, 1989
Central Equatorial Pacific (HNLC)	3.9	Blain et al., 1997
North Pacific (OSP)	5.1	Wong and Matar, 1999*
North Atlantic (POMME)	1.7	Leblanc et al., 2005b
North Atlantic (Bengal)	0.9	Ragueneau et al., 2000
Mediterranean Sea (SOFI)	0.8	Leblanc et al., 2003
Oligotrophic area		
BIO SOPE: South Eastern Pacific Gyre	0.04 (GYR) – 0.2 (EGY)	<i>This study</i>
Central Equatorial Pacific	0.8 – 2.1	Blain et al., 1997
Eastern Equatorial Pacific	0.2 – 2.5	Leynaert et al., 2001 ; Adjou et al., 2011 ; Krause et al., 2011, Demarest et al., 2011
Central North Pacific	0.5 – 2.9	Brzezinski et al., 1998
North Pacific Subtropical Gyre	0.1 – 1.7	Krause et al., 2013
North Pacific Subtropical Gyre (ALOHA)	0.1 – 0.5	Brzezinski et al., 2011
Sargasso Sea	0.5	Brzezinski and Nelson, 1995
Sargasso Sea (BATS)	0.1 – 0.9	Brzezinski and Kosman, 1996 (1996), Nelson and Brzezinski, 1997



926

 927 **Table 5: Summary of Σ B*Si* stocks in mmol Si m⁻² for the OUTPACE and BIOSOPE and other**
 928 **oceanic and oligotrophic systems.**

929

930

931

932

933

934

935

936

937

938

939

940

Region	Average Integrated Si biomass Σ B <i>Si</i> (mmol m ⁻²)	References
Coastal upwellings		
BIOSOPE: Peru-Chile upwelling	65.7 ± 53.8	<i>This study</i>
Southern California Current coastal waters	53.2 ± 39.3	Krause et al., 2015
Oceanic area		
Southern California Current oceanic waters	1.6 ± 0.3	Krause et al., 2015
BIOSOPE: South Eastern Pacific (HNLC)	11.9 ± 10.9	<i>This study</i>
Oligotrophic area		
Mediterranean Sea (BOUM)	1.1 – 28.2	Crombet et al., 2011
Sargasso Sea (BATS)	4.0 ± 6.8	Nelson et al., 1995
Sargasso Sea	0.9 – 6.1	Krause et al., 2017
North Pacific Subtropical Gyre	1.6 – 12.8	Krause et al., 2013
North Pacific Subtropical Gyre (ALOHA)	3.0 ± 1.1	Brzezinski et al., 2011
Central North Pacific	7.1 ± 3.0	Brzezinski et al., 1998
Eastern Equatorial Pacific	3.8 – 18.0	Krause et al., 2011
BIOSOPE: South Eastern Pacific Gyre	1.1 ± 1.1	<i>This study</i>
OUTPACE: South Western Pacific Gyre	1.0 ± 0.2	<i>This study</i>
OUTPACE: Melanesian Archipelago	2.4 ± 1.0	<i>This study</i>



941

 942 **Table 6: Summary of Si export fluxes in sediment traps at various depths in $\mu\text{mol Si m}^{-2} \text{d}^{-1}$**
 943 **for the OUTPACE cruise compared to other studies.**

Region	Sediment trap depth (m)	Average Si export fluxes ($\mu\text{mol m}^{-2} \text{d}^{-1}$)	References
Coastal upwellings			
Southern California Current coastal waters	100	$8,000 \pm 5,760$	Krause et al., 2015
Oceanic area			
North Atlantic (NABE)	400	10 – 145	Honjo and Manganini, 1993
North Atlantic (POMME)	400	2 - 316	Mosseri et al., 2005 ; Leblanc et al., 2005b
North Pacific Subtropical Gyre (ALOHA)	150	14 - 300	Brzezinski et al., 2011
Oligotrophic area			
Sargasso Sea (BATS)	150	17 - 700	Nelson et al., 1995
Sargasso Sea (BATS)	150	130	Brzezinski and Nelson, 1995
	200	113	
	300	85	
	300	85	
OUTPACE: South Western Pacific Gyre	153	1.8	<i>This study</i>
	328	0.5	
OUTPACE: Melanesian Archipelago	153	1.6	<i>This study</i>
	328	1.6	
	519	2.5	

944

945

946 **15 Appendices**

Stations	Σ B <i>Si</i> 0.2-2 μ m (mmol m ⁻²)	Σ B <i>Si</i> 2-10 μ m (mmol m ⁻²)	Σ B <i>Si</i> >10 μ m (mmol m ⁻²)	Total Σ B <i>Si</i> (mmol m ⁻²)
MAR1	0.36	3.49	20.28	24.12
NUK1	0.34	0.66	2.40	3.40
HNL1	0.20	2.34	5.54	8.09
1				3.79
2				0.40
3				0.48
4				0.31
5				0.20
6				0.18
7				0.20
8				0.49
GYR2	0.30	0.37	0.55	1.23
GYR5	0.13	0.24	0.39	0.75
11				0.42
12				0.82
13				0.16
14				0.47
15				1.03
EGY2	0.29	0.45	0.87	1.60
EGY4	0.15	0.25	0.65	1.05
17				2.36
18				2.47
19				0.45
20				1.50
21				3.48
UPW1*	1.27	5.36	55.43	62.05
UPW2	3.75	15.28	124.10	142.81
UPX1**	7.66	9.80	14.64	32.00
UPX2**	2.27	8.12	15.49	25.88

947

 948 **Appendix 1: Integrated size-fractionated Biogenic Silica concentrations (Σ B*Si*) in the South Eastern Pacific (BIOSOPE**
 949 **cruise) over 0-125 m. 0-50 m for * and 0-100 m for **.**

950



Stations	$\Sigma\text{BSi } 0.4\text{-}3 \mu\text{m}$ (mmol m ⁻²)	$\Sigma\text{BSi } > 3 \mu\text{m}$ (mmol m ⁻²)	Total ΣBSi (mmol m ⁻²)
1	1.24	2.52	3.76
2	0.39	3.56	3.95
3	0.43	1.83	2.26
A	0.26	1.83	2.09
4	1.06	2.24	3.30
5	0.51	3.60	4.11
6	0.70	1.80	2.49
7	0.39	1.95	2.34
8	0.39	1.12	1.51
9	0.50	1.45	1.96
10	0.77	0.98	1.75
11	0.24	1.00	1.24
12	0.17	1.29	1.46
B	0.30	1.60	1.89
13	0.17	0.96	1.13
C*	0.50	0.93	1.43
C*	0.59	1.03	1.61
14*	0.68	1.02	1.70
15*	0.76	1.38	2.14

951

952

953

Appendix 2: Integrated size-fractionated Biogenic Silica concentrations (ΣBSi) in the South Western Pacific (OUTPACE cruise) over 0-125 m and 0-200 m for *.

954

955



STATION	1	2	3	A	A	A	A	4	5	6	7	8	9	10	11	12	B	B	B	B	C	C	C	C	14	15			
Date	22/02	23/02	24/02	26/02	27/02	28/02	1/3	2/3	4/3	5/3	6/3	7/3	8/3	9/3	10/3	11/3	12/3	15/3	16/3	17/3	18/3	19/3	23/3	24/3	25/3	26/3	27/3	29/3	30/3
Diatoms																													
<i>Asterolampra marylandica</i>																													
<i>Asteromphalus heptactis/roperianus</i>																													
<i>Bacillaria paxillifera</i>																													
<i>Bacteriastrum comosum</i>																													
<i>Bacteriastrum elongatum</i>																													
<i>Ceratulina cf. pelagica</i>																													
<i>Chaetoceros hyalochaetae</i> spp/																													
<i>Chaetoceros compressus</i> with <i>Richelia</i>																													
<i>Chaetoceros dadayi</i>																													
<i>Chaetoceros peruvianus</i>																													
<i>Climacodium frauenfeldianum</i>																													
<i>Cylindrotheca closterium</i>																													
<i>Dactyliosolen blavyanus</i>																													
<i>Dactyliosolen fragilissimus</i>																													
<i>Dactyliosolen phuketensis</i>																													
<i>Ditylum brightwellii</i>																													
<i>Goslerella tropica</i>																													
<i>Guinardia cylindrus</i> with <i>Richelia</i>																													
<i>Guinardia striata</i>																													
<i>Haslea</i> sp.																													
<i>Helicotheca tamesis</i>																													
<i>Hemiaulus membranaceus</i>																													
<i>Hemiaulus haukii</i>																													
<i>Hemidiscus</i> sp.																													
<i>Leptocylindrus mediterraneus</i>																													
<i>Lioloma pacificum</i>																													
<i>Navicula/Nitzschia/Mastogloia</i>																													
<i>Nitzschia longissima</i>																													
<i>Planktoniella sol</i>																													
<i>Proboscia alata</i>																													
<i>Pseudoguinardia recta</i>																													
<i>Pseudolenia calcar-avis</i>																													
<i>Pseudo-nitzschia</i>																													
<i>Rhizosolenia</i> sp. with <i>Richelia</i>																													
<i>Rhizosolenia imbricata/bergonii</i>																													
<i>Rhizosolenia formosa</i>																													
<i>Skeletonema</i> sp.																													
<i>Stephanopyxis</i> sp.																													
<i>Thalassionema</i> sp.																													
<i>Triceratium</i> sp.																													
Undetermined pennates < 50 µm																													
Undetermined pennates 100-200 µm																													
Undetermined pennates > 200 µm																													
<i>Thalassiosira</i> -like ~15 µm																													
<i>Thalassiosira</i> -like ~50 µm																													
<i>Thalassiosira</i> -like ~100 µm																													
Radiolarians																													
Single radiolarians																													
Colonial radiolarians																													
Silicoflagellates																													
<i>Dictyocha speculum</i>																													
Diazotrophs																													
<i>Trichodesmium</i> spp.																													
<i>Richelia intracellularis</i>																													
<i>Crocosphaera</i> sp.																													
Other filamentous cyanobacteria																													

956

957

958

959

960

Appendix 3: Semi-quantitative contribution of siliceous plankton (diatoms, radiolarians, silicoflagellates) and diazotrophs in plankton nets hauls of 35 µm mesh size (over 0-150 m at all sites except but over 0-200 m at stations 14 and 15) during the OUTPACE cruise. Long duration stations were sampled every day. Light grey, medium grey and dark grey correspond to minor, common and dominant abundances respectively.

961

962



Figure 1

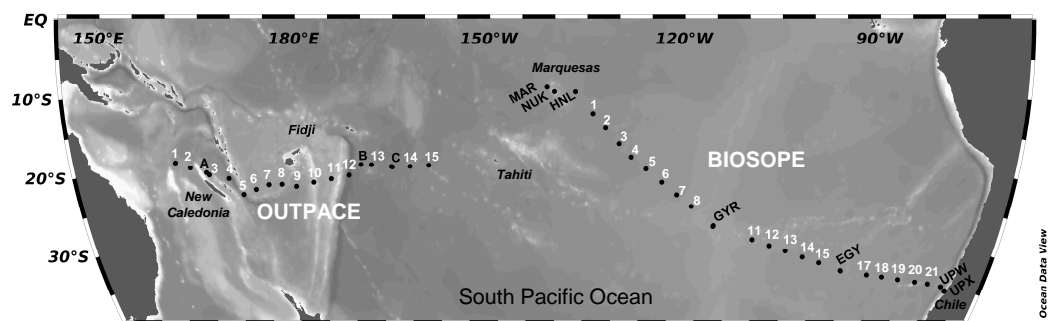




Figure 2

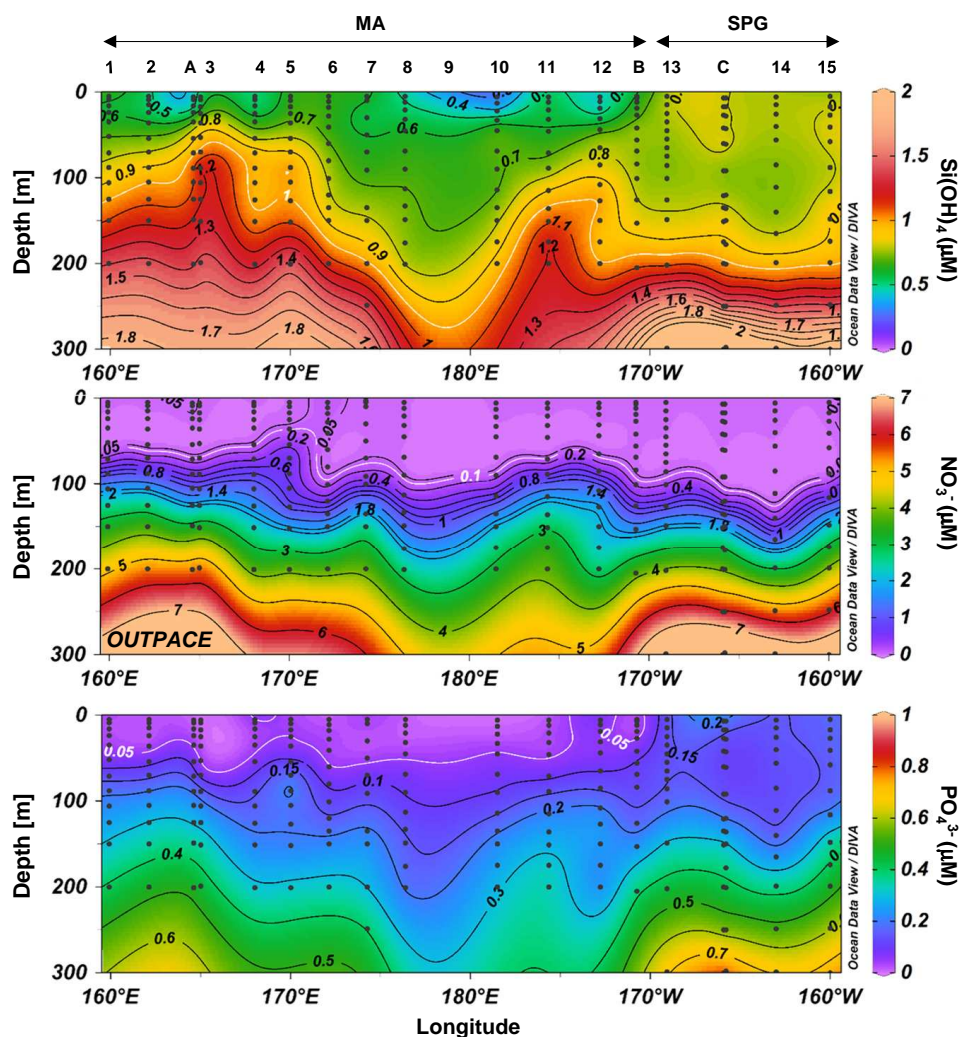




Figure 3

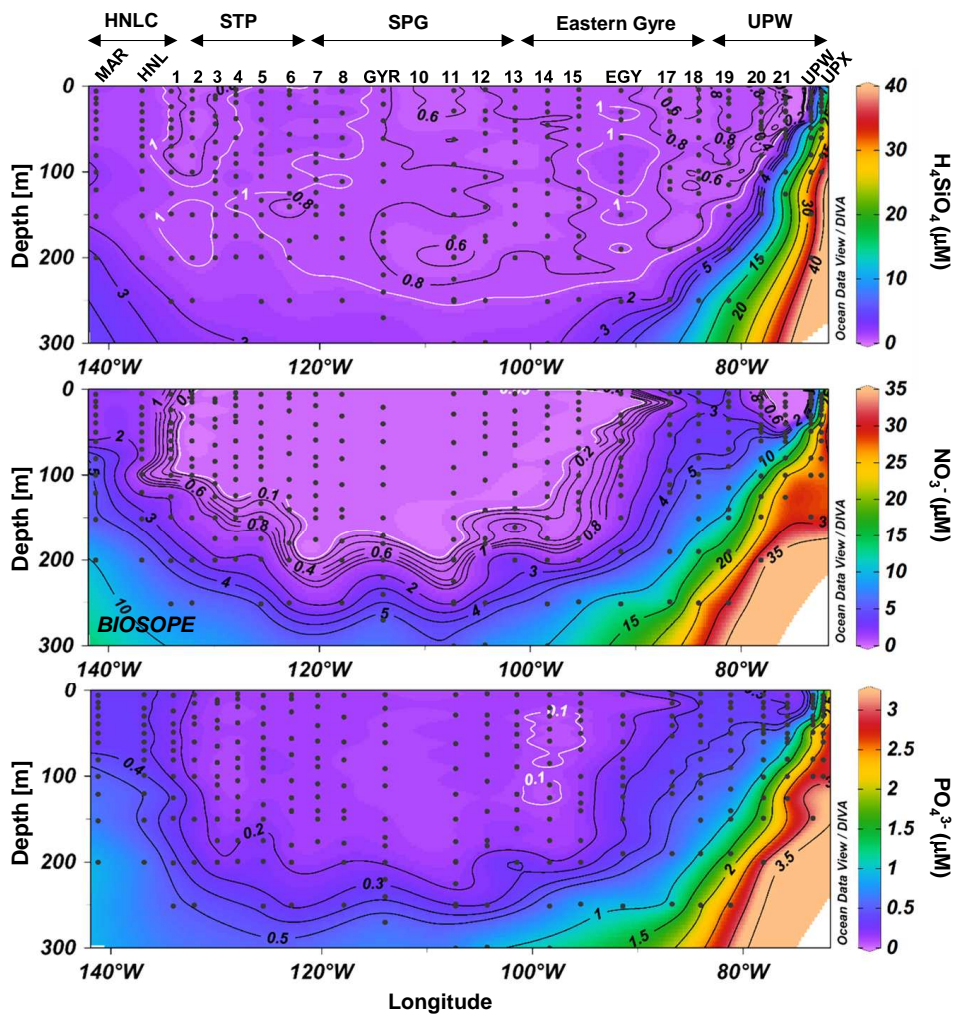




Figure 4

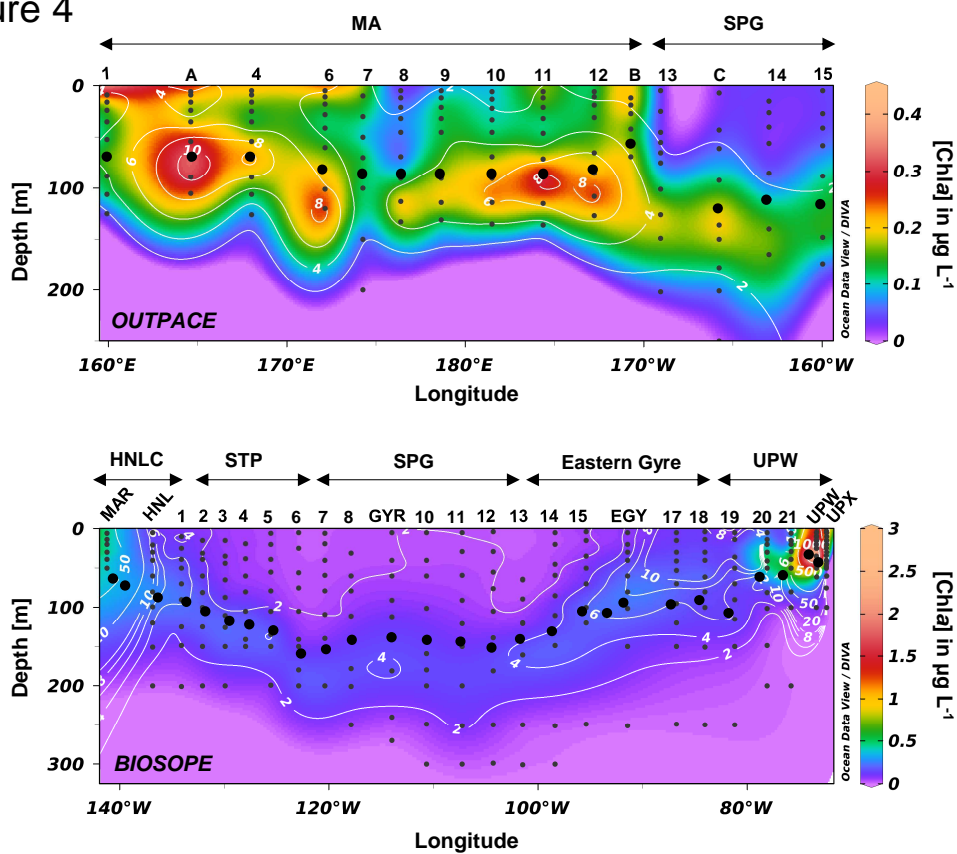




Figure 5

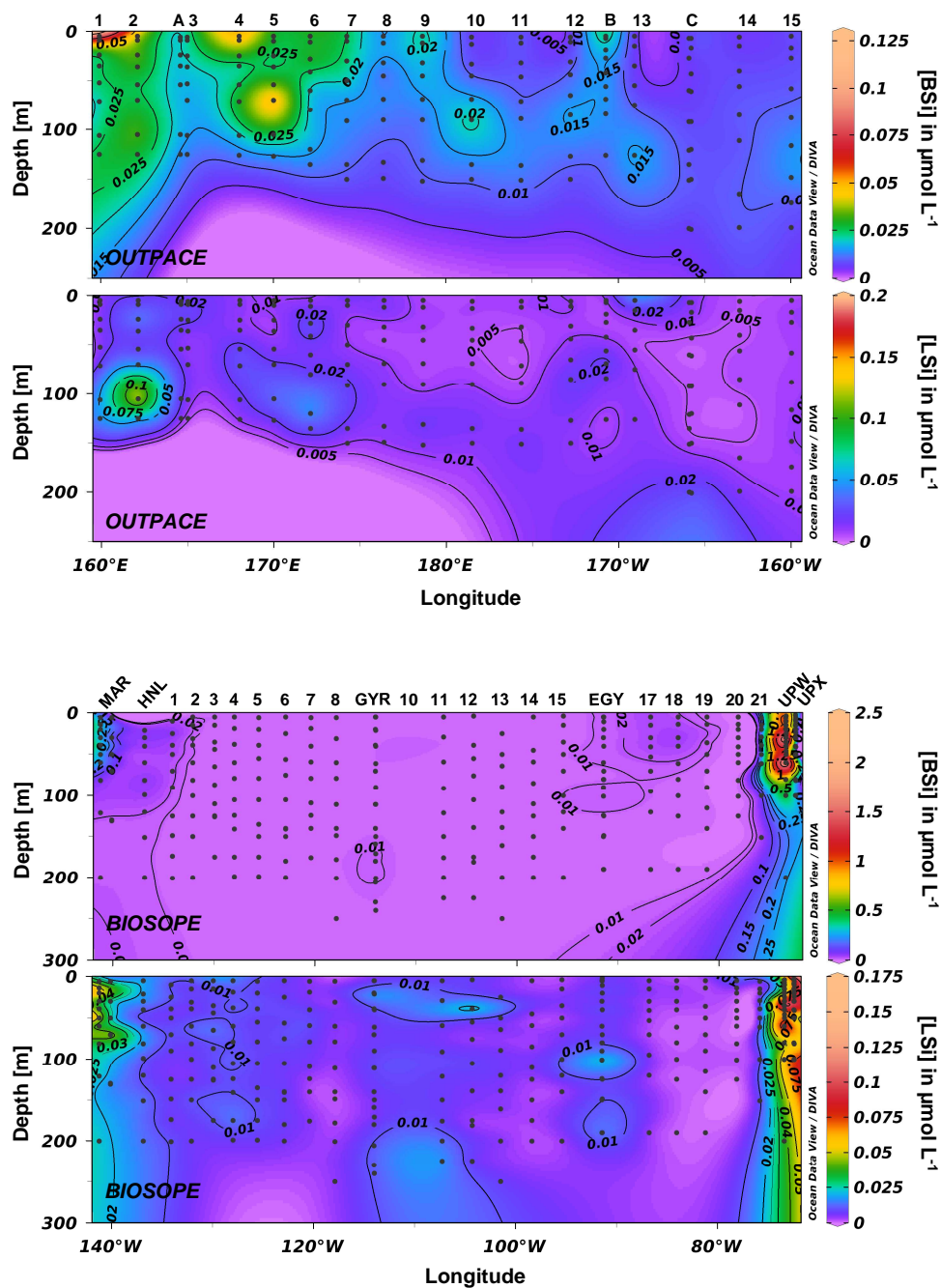




Figure 6

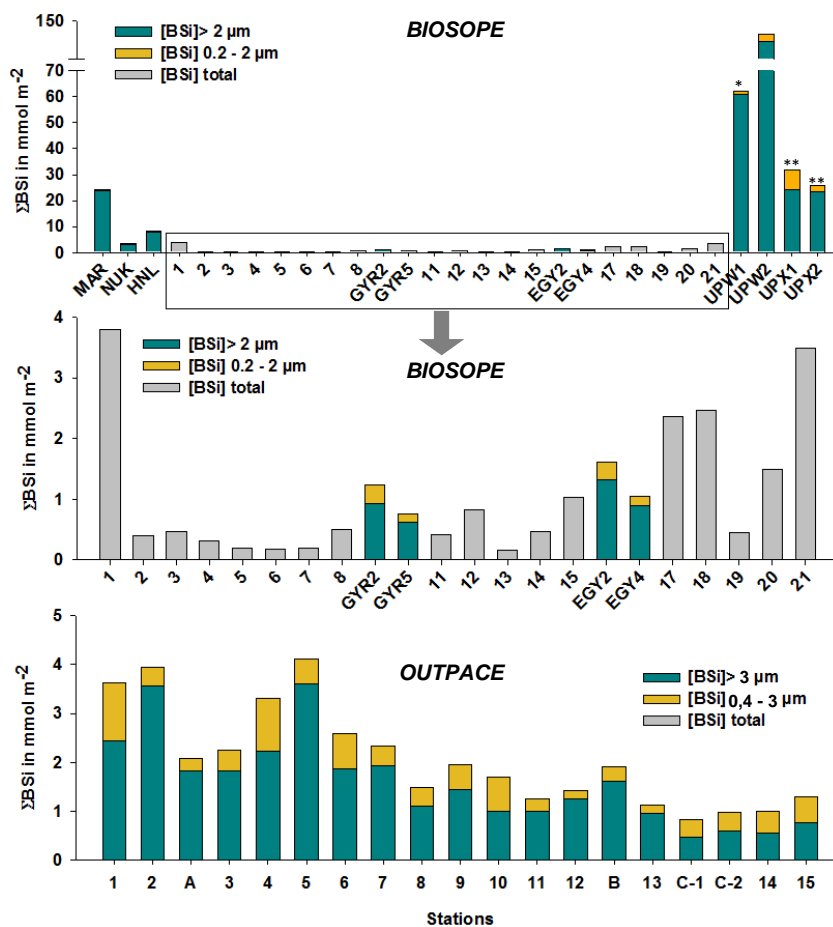




Figure 7

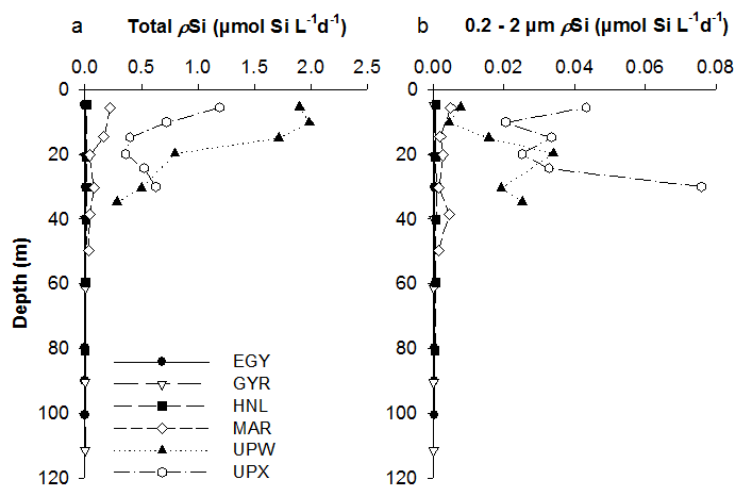




Figure 8

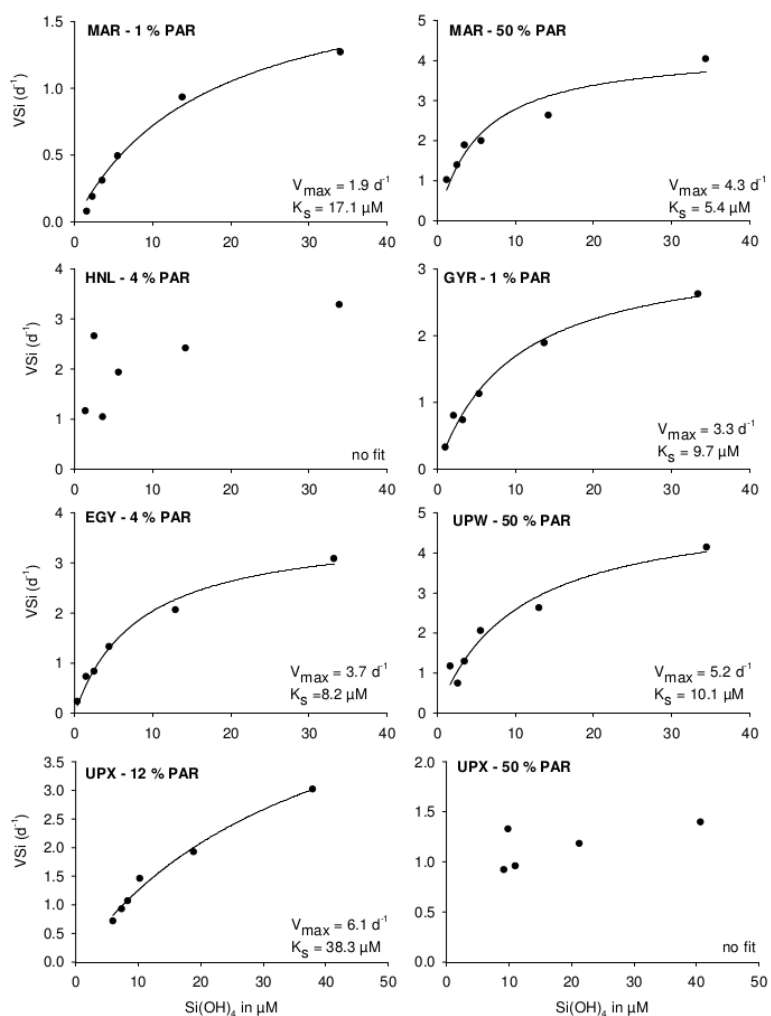




Figure 9

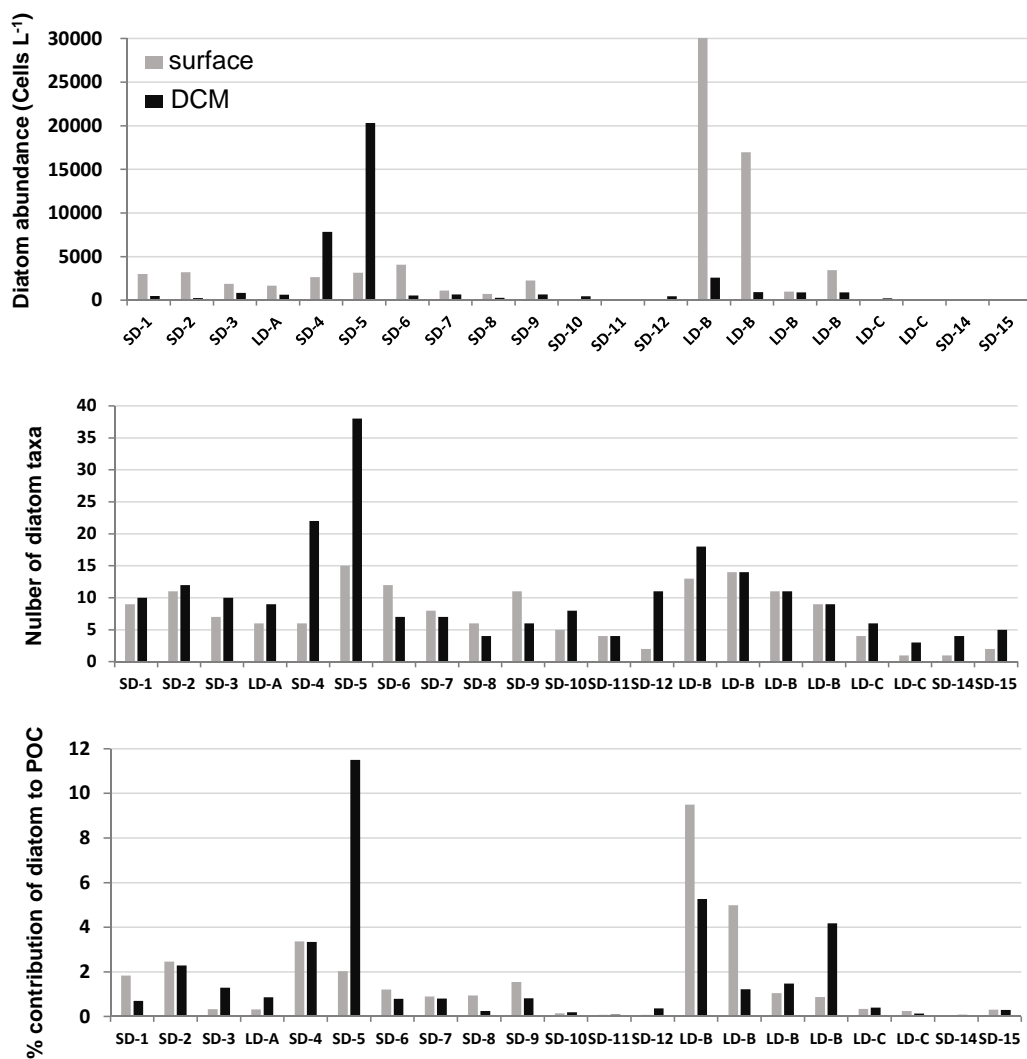




Figure 10

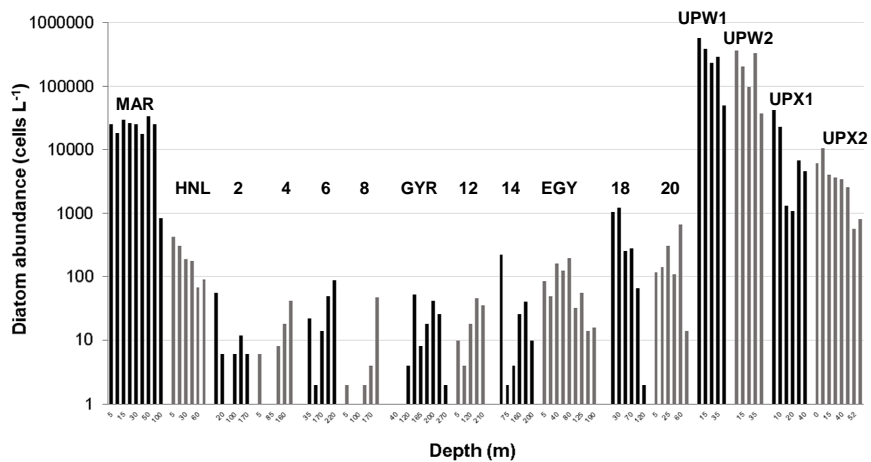




Figure 11

